2019

HOLOCENE HYDROCLIMATIC AND VEGETATION RECONSTRUCTION IN THE SIERRA NEVADA USING POLLEN AND STABLE ISOTOPES FROM CONVICT LAKE

Morgan Black
University of Kentucky, mkbl227@uky.edu
Author ORCID Identifier:
https://orcid.org/0000-0002-1258-7852
Digital Object Identifier: https://doi.org/10.13023/etd.2019.439

STUDENT AGREEMENT:

I represent that my thesis or dissertation and abstract are my original work. Proper attribution has been given to all outside sources. I understand that I am solely responsible for obtaining any needed copyright permissions. I have obtained needed written permission statement(s) from the owner(s) of each third-party copyrighted matter to be included in my work, allowing electronic distribution (if such use is not permitted by the fair use doctrine) which will be submitted to UKnowledge as Additional File.

I hereby grant to The University of Kentucky and its agents the irrevocable, non-exclusive, and royalty-free license to archive and make accessible my work in whole or in part in all forms of media, now or hereafter known. I agree that the document mentioned above may be made available immediately for worldwide access unless an embargo applies.

I retain all other ownership rights to the copyright of my work. I also retain the right to use in future works (such as articles or books) all or part of my work. I understand that I am free to register the copyright to my work.

REVIEW, APPROVAL AND ACCEPTANCE

The document mentioned above has been reviewed and accepted by the student's advisor, on behalf of the advisory committee, and by the Director of Graduate Studies (DGS), on behalf of the program; we verify that this is the final, approved version of the student's thesis including all changes required by the advisory committee. The undersigned agree to abide by the statements above.

Morgan Black, Student

Dr. Michael McGlue, Major Professor

Dr. Edward W. Woolery, Director of Graduate Studies

HOLOCENE HYDROCLIMATIC AND VEGETATION RECONSTRUCTION IN THE SIERRA NEVADA USING POLLEN AND STABLE ISOTOPES FROM CONVICT LAKE

THESIS

A thesis submitted in partial fulfillment of the
requirements for the degree of Master of Science in the
College of Arts and Sciences
at the University of Kentucky

By

Morgan Katherine Black

Lexington, Kentucky

Director: Dr. Michael McGlue, Professor of Earth and Environmental Sciences

Lexington, Kentucky

2019

https://orcid.org/0000-0002-1258-7852

ABSTRACT OF THESIS

HOLOCENE HYDROCLIMATIC AND VEGETATION RECONSTRUCTION IN THE SIERRA NEVADA USING POLLEN AND STABLE ISOTOPES FROM CONVICT LAKE

The forested environments of the subalpine and upper montane zones of the eastern Sierra Nevada mountains (California) are biodiverse and valuable ecosystems that are sensitive to hydroclimate changes. The history of high-altitude vegetation changes in the eastern Sierra Nevada is underexplored, and this knowledge gap can be addressed using a paleolimnological approach. In this study, we use a long (~9.5 m) sediment core from Convict Lake, a glacial lake situated in the upper montane zone of California's Sherwin Range, to assess Holocene changes in terrestrial vegetation. The core was dated using radiocarbon, and studied with palynology, elemental analysis, and stable isotope geochemistry applied to bulk organic matter. Pollen assemblages provide evidence of a dry, open woodland in the Convict Creek watershed during the early Holocene, while the data indicate a stable, cool, and relatively wet mid-Holocene with subalpine forests occurring at lower elevations. All datasets point to considerable hydroclimatic variability beginning around 4,500 yr B.P., which may reflect warmer temperatures and more variable winter precipitation. The presence of the subalpine indicator species *Tsuga mertensiana* coincides with potential late Holocene glacial advances for which scant evidence currently exists. New insights from this study provide crucial baseline data for comparison with climate simulations of the future for the Sierra Nevada, which serve as the most important water source for vast urban and agricultural areas in California and provide millions of dollars in economic revenue annually.

KEYWORDS: Intertropical Convergence Zone, Glacial Advance, Montane Forest, Paleoclimate, Snowpack, Subalpine

Morgan Katherine Black

(Name of Student)

9/5/2019

Date

HOLOCENE HYDROCLIMATIC AND VEGETATION RECONSTRUCTION IN THE SIERRA NEVADA USING POLLEN AND STABLE ISOTOPES FROM CONVICT LAKE

By

Morgan Katherine Black

Dr. Michael McGlue
Director of Thesis

Dr. Edward Woolery
Director of Graduate Studies

9/5/2019
Date

DEDICATION

This thesis is dedicated to my entire family.

Special dedication is to my grandmother, Nada Earlene Hensley, a dairy farmer and school bus driver who taught me how to have grit, and to work until the job was done.

Special dedication is to my mother and father, who have been beacons of light in my life. You have taught me many things, but most importantly, you taught me to persevere. This lesson alone is why I have succeeded.

Special dedication is also deserved by Clayton Gullet, who has loved me and sacrificed on my behalf, beyond expectation

ACKNOWLEDGMENTS

This work would not have been possible if not for the invaluable input received from both my advisor, Dr. Michael McGlue, and Dr. Sarah Ivory. You both have provided me with time, energy, and resources that you did not have to. I will always appreciate this. Dr. Ryan Thigpen has provided me with professional and personal advice that I will carry with me far into the future.

I have also received indispensable assistance in the field, the lab, and in life, from Laura Streib, Bailee Hodelka, Joseph Lucas, and Eva Lyon. You all have made me laugh and have provided hugs when I've cried. The friendships I have formed with you are equally as valuable to me as the title I will have earned.

TABLE OF CONTENTS

LIST OF TABLES

LIST OF FIGURES

1. Introduction

Paleolimnological studies on lakes situated in the rain shadow of the Sierra Nevada have revealed a complex environmental history, especially during the late Holocene (Lajoie, 1963; Anderson 1990; Stine, 1990; Davis, 1999; Zimmerman et al., in review). These studies have been valuable for understanding millennial-scale controls on mountain climate and hydrology in an area that is critical to California's water supply. On a comparative basis, far less is known about the history of terrestrial biomes on the eastern side of the Sierra Nevada since the last deglaciation. New research on other lake records in the Sierra Nevada, specifically those located at higher altitudes, are therefore essential to achieve a better understanding California's subalpine and montane forest development through time. This information is important because subalpine and upper montane forests are one of most economically viable ecosystems in California, and one of the most biodiverse temperate conifer forests in the world (Fites-Kaufman et al., 2007). Prior to ~1950 CE, these forests were valued for their timber, and considerable harvesting of ponderosa and Jeffrey pine trees took place east of the Sierran crest to support growing communities and mining operations elsewhere in California (Laudenslayer and Darr, 1990; McKelvey and Johnston, 1992). Today, the protected wilderness areas in Inyo County, California, where these forests thrive, generate $499 million USD annually in economic benefit for the eastern Sierran region through tourism and the subsequent consumer dollars spent in neighboring communities for services such as lodging (Richardson, 2002).

Montane forests in this region are defined as mixed conifer forests that are most often characterized by the presence of *Abies magnifica*, *Pinus jeffreyi*, *Pinus monophylla*, *Populus tremuloides, Ceanothus, Quercus vacciniola, Cercocarpus, Artemisia* spp. (mugworts, wormwood, sagebrush) and *Erigonum* (wild buckthorn) (Fites-Kaufman et al., 2007). These forests are highly dependent on seasonal drought and fire to maintain stability and health (Fites-Kaufman et al., 2007). Fundamentally, the ecosystem dynamics of these forests in response to climatic forcing is not well understood, despite the clear importance of these plant communities for ecosystem diversity and habitat in the Sierras (North et al., 2016). The elevation limits for the border between upper montane and subalpine forests provide a unique proxy for analyzing snowpack trends in the Sierras because increases in snowpack are related to lower elevation limits for the transition between the two forests types (North et al., 2016). The snowpack and its interannual variability stand as one of the most closely tracked environmental conditions in the Sierras, due to the importance of winter snowfall for mountain ecology, stream hydrology, and fisheries management (e.g., Maciolek and Needham, 1952; Erman et al., 2011). Knowledge of snowpack trends in the eastern Sierra is critical; snowmelt supplies a seasonal freshwater pulse to the Owens River and Mono Lake basins, which are connected via the Los Angeles Aqueduct system and provide nearly a third of all water used by Los Angeles County (Bales et al., 2018). Herbst and Cooper (2010) noted the importance of winter precipitation falling as snow rather than rain, because a decrease in precipitation falling as snow results in lower snow water storage and increases the potential for early runoff, damaging floods, and loss or conversion of montane habitat as snowlines rise.

The eastern Sierra snowpack is particularly vulnerable to warming. It has been noted by the Intergovernmental Panel on Climate Change (IPCC) that the evidence of observed impacts of climate change are strongest in natural systems, for example changing precipitation and early snow melt are affecting the quality and quantity of water resources (IPCC, 2014). The IPCC also reports in very high confidence that snow cover in the Northern Hemisphere has decreased by 0.8 – 2.4 % per decade since the mid-20th century in the months of March and April, and 11.7% per decade for the month of June (IPCC, 2014). It is very likely that that there are anthropogenic influences on the observed reduction in Northern Hemisphere spring snow cover since 1970, but how the snowpack will change in the future remains an open question (IPCC, 2014). It has been predicted that an earlier snowmelt of one month will occur with a mean temperature increase of just 2°C (Bales et al., 2018). Early melting is associated with warm winters, which portends a shorter time span for snow to accumulate and a fundamental limit on the snow water equivalent that feeds reservoirs, recharges groundwater, and supports the growing season of the vast agricultural industry on the western side of the Sierras in the San Joaquin valley (Bales et al., 2006). Bales et al. (2018) also predicts that a mean temperature rise of 6°C would result in a near total loss of snow accumulation. Predictions using vegetation data from satellite and aircraft surveys in support of hydrologic data and modeling are critical to understanding how snow accumulates, and historical vegetation data will further improve predictions of this kind.

One important resource for learning more about the history of forests in the Sierra Nevada mountains is through pollen extracted from well-dated lake sediments. Palynological analyses have been completed on a number of lake sediment sequences at

relatively low altitudes in the Sierra Nevada region, but studies from the subalpine and montane zones are much less common (Adam, 1967; Betchelder, 1980; Adam and West, 1983; Anderson et al., 1985; Davis et al., 1985, Adam, 1988; Anderson, 1990). To address the knowledge gap surrounding the history of montane forests in the eastern Sierra Nevada during the Holocene, this study adopted a paleolimnological approach focusing on the strata of Convict Lake, a high-altitude, hydrologically-open glacial lake ~48 km southeast of Mono Lake in the eastern Sierra Nevada (Figure 1). Here, we present an analysis of the last 9,500 yrs of vegetation change using a new radiocarbon-dated sediment core collected from Convict Lake. Convict Lake is situated behind a series of spectacular late Pleistocene-aged terminal moraines within Convict Creek canyon in the Sherwin Range (Greene and Stevens, 2002). The Sherwin Range is an important subrange of the Sierra Nevada located in Mono County, California. According to the Mono County Community Development Department (MCCDD), the Sherwin Range snowpack is the main source of freshwater input for Lake Crowley, a natural lake-turned-reservoir that provides a stable water and power resource for Los Angeles County (MCCDD, 2007). A multi-indicator analysis that included pollen analysis, elemental and stable isotope geochemistry was used to infer Holocene fluctuations in aquatic environments, hydroclimate, and changes in subalpine and upper montane forests in the surrounding area. These data provide new insights on the Holocene history of forests in the Sherwin Range.

Understanding forest response to climatic shift at various altitudes will help us understand the future of the Sierra Nevada snowpack, as well as the ecological shifts that have begun to occur as the Earth has rapidly warmed and human develop projects have

encroached into mountain environments (Cayan et al., 2009). Armed with this knowledge, decision makers will be more prepared to address potential climate impacts on dense population centers in the future, such as highly altered hydrology and water availability (Climate Resilience Toolkit, U.S. Federal Government, 2014).

1.1 Study Location

Convict Lake (37.5899° N, 118.8582° W) is located within Convict Creek drainage basin, which is a part of the Sherwin Range in the eastern Sierra Nevada (Figure 1). The limnology of Convict Lake and the Convict Creek drainage basin has not been extensively studied since the 1940-1950s (Reimers et al. (1955)). At that time, the lakes of the Convict Creek watershed were analyzed to gain environmental and limnological data to inform fisheries management. There are ten lakes in the Convict Creek watershed, nine of which are located upstream and are connected to Convict Lake via Convict Creek (Figure 2). All the lakes in the drainage basin are relatively young, having formed following the last glacial cycle (Reimers et al., 1955). The headwaters of Convict Creek are on the north slopes of Red Slade Mountain (4,012 m.a.s.l), where there are numerous small glaciers and rock glaciers (MCCDD, 2007). At 3,823 m.a.s.l, a major tributary enters Convict Creek from the west, which drains several lakes on the east side of Bloody Mountain (MCCDD, 2007). There is a stream gauge maintained by the United States Geological Survey located at 2,270 m.a.s.l and 3 km upstream from highway 395 (MCCDD, 2007). Streamflow averages 10 cfs in the winter and 100 – 120 cfs during the spring and summer months, when snowmelt peaks (MCCDD, 2007). Convict Creek feeds into Convict Lake from the southwest and forms a prominent delta that delivers sediment

offshore (McGlue and Woolery, submitted). Convict Creek flows out from the northwest axis of Convict Lake and ultimately drains into Lake Crowley.

Today, Convict Lake covers a surface area of ~ 0.68 km^2, is ~ 44 m deep at its depocenter, and has a shoreline elevation of ~ 2,393 m.a.sl. It is a hydrologically open lake whose water balance appears to be strongly influenced by the seasonal melting of snowpack (Reimers et al., 1955). Blackwelder (1931) and Reimers et al. (1955) both indicate that Convict Lake's origins are tied to the last glaciation and that it is best classified as a terminal moraine lake. Terminal moraine lakes are the result of a moraine effectively damming a drainage basin (Cohen, 2003). These lakes are often successfully developed when there is an existing excavated valley to then infill with glacial meltwater and outwash, which is the case for the Convict Creek valley.

Convict Lake is dimitic and covered by ice from December to May (Reimers et al., 1955). Reimers et al. (1995) observed that deep water mixing occurs in the autumn and spring, while the water column remains thermally stratified during the summer. Water chemistry data gathered by Reimers et al (1955) demonstrates that the lake water is Ca^{2+} - K^{+} - HCO_3^{-} rich. Melack et al. (1985) affirms the dominance of Ca^{2+} and HCO_3^{-}, but reports higher concentrations of Na^{+} than K^{+}. The transparency value is 15.5 m and suggests that the lake is oligotrophic, thus it can be inferred that the net primary production of such a lake ranges from 500-300 mg C/m^2/d (Wetzel, 2001).

A bathymetric map produced by McGlue and Woolery (submitted) reveals that Convict Lake has a flat and extensive deepwater depocenter, where water depths routinely exceed 37 m and reach a maximum of ~44 m. McGlue and Woolery (submitted) noted that the lake has steep slopes along lateral basin margins, an

asymmetric deltaic ramp on the southwest axial margin, and a moderate gradient littoral ramp that shoals toward the lake outlet, where Convict Creek exits toward Lake Crowley. This information was used to help guide the selection of the coring sites reported on in the present study.

1.2 Geology

Convict Lake is found within the Mount Morrison roof pendant, which consists of middle Cambrian to middle Permian metasedimentary rocks that are underlain by Triassic and Jurassic metavolcanic rocks (Greene and Stevens, 2002). Convict Lake is known for the colorful outcrop exposures along its margins, specifically the Sevehah Cliffs and Laurel Mountain (Figure 1B); the natural scenic beauty of the lake has led to some human development, including a spillway over the Convict Creek outlet, a small marina on the northeastern axial margin, and a well-used hiking trail that circles the lake. The Sevehah Cliffs and Laurel Mountain exposures contain most of the stratigraphic units and important structures in the Mount Morrison pendant. Key formations include the Cambrian-Lower Ordovician Mount Aggie Formation, the Ordovician Convict Lake Formation and the Upper Devonian Sevehah Group. The Mount Aggie and Convict Lake Formations are primarily dark-colored, organic rich, fine-grained mudstones that weather easily and contributed to the sediment package found along Convict Lake's subaqueous margins via avalanching (McGlue and Woolery, submitted). The Mount Aggie Formation also contains crystalline limestone in the Salty Peterson member, which could potentially influence lake chemistry and sedimentary carbonate content during intervals of peak discharge from Convict Creek (Green and Stevens, 2002).

There is an abundance of shallow seismic activity in the Convict Creek watershed, with 53 earthquakes of ≥ 4.5 magnitude since 1940 CE (http://www.ncedc.org/ncss/) (McGlue and Woolery, submitted). The steeply dipping Laurel-Convict Fault runs through the Sevehah Cliffs (Greene and Stevens, 2002). This northwest-striking fault cuts bedding in the upper Paleozoic rocks at a low angle, and cuts obliquely across folds and faults in the lower Paleozoic rocks (Greene and Stevens, 2002). The Long Valley Caldera is just 26 km north of Convict Lake and likely influences earthquake activity across the region. Holocene rhyolitic volcanism of the Long Valley Caldera is a likely source of tephras found within the cores recovered from Convict Lake.

1.3 Glacial History

The entirety of the Sierra Nevada range was extensively glaciated throughout the Pleistocene, with small glaciers remaining in sheltered cirques today (Gillespie and Clark, 2011). These cycles of Pleistocene glaciation gave rise to multiple present-day ice scour lakes, such as June and Gull lakes (Lyon et al., 2019). There are approximately 13 recognized Quaternary glaciations for the Sierra Nevada (Gillespie and Clark, 2011). There are six terminal moraines surrounding Convict Lake, including the pre-Tahoe (220-140 kyr B.P.), Mono Basin (80-60 kyr B.P.), Tahoe (50-42 kyr B.P.), Tenaya (31 kyr B.P.), Tioga (25-16 kyr B.P.), and latest Tioga (14- 15 kyr B.P.) (Gillespie and Clark, 2011). After the latest Tioga, the next recorded ice advance is the Recess Peak glaciation, which most evidence suggests to have occurred ~14.2-13.1 kyr B.P. (Clark, 1997, Phillips et al., 2009, Gillespie and Clark, 2011). The only extensive Holocene glaciers

that have been recorded are the Matthes glaciers, which reached their maximum 600-700 yr B.P., coeval with the Little Ice Age (LIA). According to Bowerman and Clark (2011), lake sediment evidence in the central Sierra Nevada for ice advances also exists for the mid-late Holocene (~3.2-2.8 kyr B.P.) as well as at ~2.2 and 1.6 kyr B.P, but few other studies report higher winter precipitation or lowered snowlines at those times.

1.4 Modern Climate and Vegetation

The eastern Sierra Nevada mountains experience a Mediterranean-type climate with hot, dry summers and cold, wet winters (Anderson and Davis, 1988). Historical climate and weather data are available from a NOAA station at Mammoth Lakes, which is < 1 km east of Convict Lake. For 2018, the average daily maximum temperature was ~ 7.8 °C in January and ~ 29 °C in July. Precipitation is winter dominated, and in 2018 Convict Lake received ~15.8 cm of rain and ~ 93.5 cm of snow and ice in the winter months. Historically, the coolest months of the year are December, January, and February, with daytime highs averaging ~ 5°C (NOAA, 2018) (Figure 3). The wettest month of the year is February, with total precipitation averaging ~6.8 cm since 1994 (Figure 3). June through September are the hottest and driest months, with average daily temperatures reaching ~ 25 °C in July, and precipitation averaging < 0.1 mm for all of summer (Figure 3).

Convict Lake is within the elevation limits for the Jeffrey pine, Juniper – Pinyon forest type (Anderson and Davis, 1988) (Figure 4). On the eastern side of the Sierran crest, forests typically transition into a Jeffrey pine (*Pinus jeffreyi*) woodland just below the subalpine and upper montane zones (Anderson and Davis, 1988). Further downslope,

the forest grades into a Pinyon Pine-western juniper assemblage with big sagebrush (*Artemisia tridentata*). Valley bottoms are characterized by a shrubby assemblage dominated by sagebrush, greasewood (*Sarcobatus vermiculatus*) and joint-fir (*Ephedra* spp.). Vegetation around Convict Lake is dominated by sagebrush, Jeffrey pine, mountain mahogany (*Cercocarpus betuloides*), aspen (*Populus* spp.), and cottonwood (*Populus fremontii*), as well as sparse wildflower growth. Within the lake, patchy growth of *Ranunuculus* and *Myriophyllum* were observed by Reimers et al. (1955) in a few sandy bottom areas. Though sparse, the green algae *Rhizoclonium* was also observed during that survey.

1.5 Modern Pollen Rain

Anderson and Davis (1988) discovered that of the nearly 100 pollen types that were observed in Sierra Nevada pollen assemblages, fewer than 25 occur regularly in modern and fossil samples. These common types include *Pinus*, *Tsuga mertensiana*, *Abies*, Taxodiaceae- Cupressaceae – Taxaceae (TCT), *Quercus*, Poaceae, Amaranthaceae, and *Artemisia*.

Anderson and Davis (1988) state that in modern samples, *Pinus* pollen abundances dominate throughout most of the elevational range. However, it is often difficult to interpret pine pollen percentages due to the ten or more species contributing to the modern pollen rain (Anderson and Davis, 1988). Anderson and Davis (1988) suggest that values below 24% indicate a local absence of pine trees, and that values above 94% can be found in assemblages in high altitudes above the modern tree line.

Tsuga mertensiana (mountain hemlock) displays a bimodal pattern in the modern pollen rain, with highest percentages found in a restricted elevation range on the west (4.2-

31.9% between 2,590 and 2,743 m a.s.l.) and east (0.7-11.7% between 2,775 and 2,866 m a.s.l.) sides of the Sierran crest, respectively (Anderson and Davis, 1988). Importantly, Anderson and Davis (1988) make clear that *Tsuga* pollen averages < 1% outside the immediate vicinity of the source, so it will not be found outside of a subalpine forest. Thus, *Tsuga* pollen presence is an important indicator of subalpine forest.

Taxodiaceae-Cupressaceae-Taxaceae includes members of the Taxodiaceae (*Sequoiadendron*), Cupressaceae (*Juniperus* and *Calocedrus*), and Taxaceae (*Taxus* and *Torreya*) families. These pollen types also exhibit a bimodal distribution with respect to elevation (Anderson and Davis, 1988). On the eastern side of the crest, Anderson and Davis (1988) reported that modern pollen samples from 2,440 – 2,622 m.a.s.l. (subalpine zone) range from 1.3 to 3.6% T-C-T pollen, all of which was Juniperus.

Ericaceae pollen was only found in abundance in one site studied by Anderson and Davis (1988), at an elevation of 700 m a.s.l., in the chaparral zone. Anderson and Davis (1988) noted that the plant must be extremely abundant to be found within a pollen transect. The chaparral zone is characterized by high abundances of buckthorn, manzanita, mountain-mahogany and a diverse array of shrubbery (Anderson and Davis, 1988).

Rhamnaceae (wild buckthorn) is most common in the openings of the Sierra montane forest and chaparral, with the pollen type following this plant's distribution (Anderson and Davis, 1988). Rhamnaceae pollen is a good indicator of relatively open forest conditions situated at mid to low elevations (up to 1900 m.a.s.l.) (Anderson and Davis, 1988)

Quercus pollen can be found in almost all modern and fossil samples within the Sierras (Anderson and Davis, 1988). *Quercus kelloggi, Q. lobata, Q. douglasii, Q.*

wisilizenii, and *Q. chrysolepsis* are typically only found in the lower elevations on the western side of the crest. On the eastern side of the Sierra crest, *Q. vaccinifolia* is the most common oak species found in the lower montane zone, and it has occasionally been found extending into the upper montane forests (Anderson and Davis, 1988). Maximum values are found in the chaparral zone of 400 – 700 m a.s.l. (Anderson and Davis, 1988).

Poaceae is only found in modern samples where there are little to no closed canopy forests (Anderson and Davis, 1988). Such environments include the chaparral zone at ~700 m.a.s.l., high elevations along the Sierran crest, and most forests on the eastern side of the crest (Anderson and Davis, 1988). This pollen type is only discernable at the family level and is indicative of an open canopy ecosystem (Anderson and Davis, 1988).

Amaranthaceae is never abundant in any of the study areas of Anderson and Davis (1988), but values do exceed 1% at 500 m a.s.l. and below on the west side of the crest and at 2,073 m.a.s.l. and below on the eastern side (Anderson and Davis, 1988). This pollen type is a good indicator of open, dry-adapted vegetation (Anderson and Davis, 1988). *Artemisia* (sagebrush, wormwood) generally occurs above 1,830 m.a.s.l., whereas some shrubby species can inhabit areas below this elevation and are indicative of an open habitat (Anderson and Davis, 1988).

1.6 Previous Research

There have been relatively few pollen studies completed in the eastern Sierra Nevada, with most of the pioneering studies having been completed using lake and meadow sediments from lower altitudes than Convict Lake (Adam, 1967; Betchelder, 1980; Adam and West, 1983; Anderson et al., 1985; Davis et al., 1985, Adam, 1988;

Anderson, 1990). Anderson (1990) completed the first high altitude pollen study east of the Sierran crest, confirming three distinct shifts in forest composition in the Holocene. Anderson (1990) notes that before 10,000 B.P., trees were absent or sparsely established on the Sierras, most likely due to poor soils following the last deglaciation. During the early Holocene (10,000-6,000 yr B.P.), *Pinus murrayana* became established at its current altitudinal range, whereas subalpine conifers were confined to the most mesic habitats (Anderson, 1990). The elevation of *Tsuga meretenisana* (mountain hemlock) and *Abies magnifica* (red fir) track precipitation changes in the early Holocene, for their current altitudinal boundaries allow for the inference of subalpine forest migration (Anderson and Davis, 1999). High-altitude forests of the Sierras were structurally different during the early Holocene than what is observed at the present time, with open-ground species like *Artemisia* and other Asteraceae being much more common in the pollen record than currently (Anderson, 1990). Paleovegetation datasets indicate that at 6,000 yr B.P., effective precipitation most likely increased in the Sierra Nevada. For example, at Tioga Pass Pond, the highest elevation lake (3,018 m.a.s.l.) in the Anderson (1990) study, the dry, herb and shrub-dominated open meadow was colonized by *P. murrayana*. Toward the end of the early Holocene, co-occurring with the increase in effective precipitation at 6,000 yr B.P., pollen evidence indicates that there was a regional scale closing of Sierra forests, as percentages of montane chaparral shrubs at lower elevation study sites decreased significantly.

Anderson (1990) also observed that cooler conditions occurred from about 3,000 to 2,500 yr B.P., as shown by a down-slope shift of the altitudinal limits of *Tsuga mertensiana* and *Abies magnifica*. An important feature of the late Holocene pollen record

for the eastern Sierras was an increase in *Abies magnifica* pollen at all sites studied in Anderson (1990), which suggests that modern high-altitude montane forests have only developed as a result of hydroclimate changes within the latest Holocene. Similarly, Mensing et al. (2004) inferred that a cool and wet climate occurred between 3,430 and 2,750 yr B.P. at Pyramid Lake (Nevada), and they suggested that Lake Tahoe began to spill over continuously at that time, thus raising the water level of the downstream Pyramid Lake.

Davis (1999) inferred a cool, dry early Holocene at Mono Lake that was marked by the presence of a thinolite tufa that spans 10,720– 10,120 yr B.P. and elevated values of Amaranthaceae pollen, indicating the development of halophytic vegetation (Davis, 1999). The mid Holocene (7,830 - 4,480 yr B.P.) was a period of relative stability in the terrestrial vegetation in the Mono Lake watershed. Davis (1999) interpreted that lake levels remained relatively high, and there was little fluctuation in the vegetation based on the pollen spectra. Late Holocene (4,480 yr B.P. – present) climate was inferred from pollen to be highly variable at Mono Lake, with three intervals of drastic vegetation change that coincide with water level lowstands at ~ 4,480, 2,480, and 1,030 yr B.P. (Davis, 1999). These lowstands are characterized by large decreases in pine pollen. Following the drought at 4,480 yr B.P., Pinus percentages exceed 80%, which are the highest values for the Davis (1999) record. This interval corresponds with Stine's (1990) Dechambeau Ranch highstand for Mono Lake, thus demonstrating that lake levels influence pollen transport and deposition (Davis, 1999). Additional evidence of this coupling includes the low-precipitation interval inferred at 2,480 yr B.P., which corresponds with Stine's (1990) Marina lowstand (Davis, 1999). Percentages of shrubs like *Artemisia*, Erigonum, Amaranthaceae, and other Asteraceae are

higher after 1,960 yr B.P., which tracked the development of the modern vegetation assemblage at Mono Basin (Davis, 1999).

In the Great Basin, the early Holocene marks the driest period in the last 7,600 yrs (Mensing et al., 2004). Mensing et al. (2004) interpreted a wetter climate in the nearby Pyramid Lake at ~ 6,300 yr B.P., which was marked by an increase in Artemisia and a decrease in Amaranthaceae. From 5,200 to 5,000 yr B.P., Mensing et al. (2004) inferred a drought in the Great Basin that is marked by an increase in Amaranthaceae, which coincides with the drought oscillation recorded by Benson et al. (2002). Benson et al. (2002) reports that during the last 7,620 cal yr the hydrologic balance in the Great Basin oscillated approximately every 150 yrs, and that during the last 2,740 yrs, drought durations have spanned 20 to 100 yr intervals and drought-free periods have spanned 80 to 230 yrs. Benson et al. (2002) also indicated that the mid-Holocene (8,000 – 3,000 yr B.P.) was mostly warm and dry for the Great Basin, and Pyramid Lake was much shallower than today.

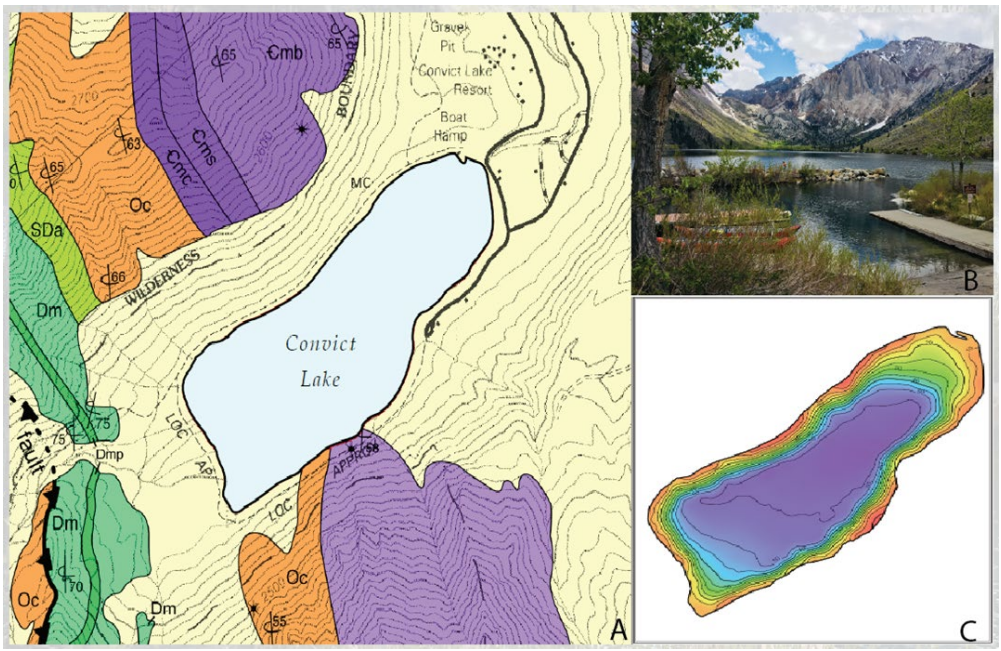

Figure 1. Panel A illustrates that Convict Lake has formed in a Quaternary glacial moraine. Several cliff faces behind the lake (panel B) including the Sevehah Cliff and Laurel Mountain expose folded and faulted Paleozoic metasedimentrary rocks (Greene and Stevens, 2002). Lake-bed bathymetry is relatively uniform (panel C).

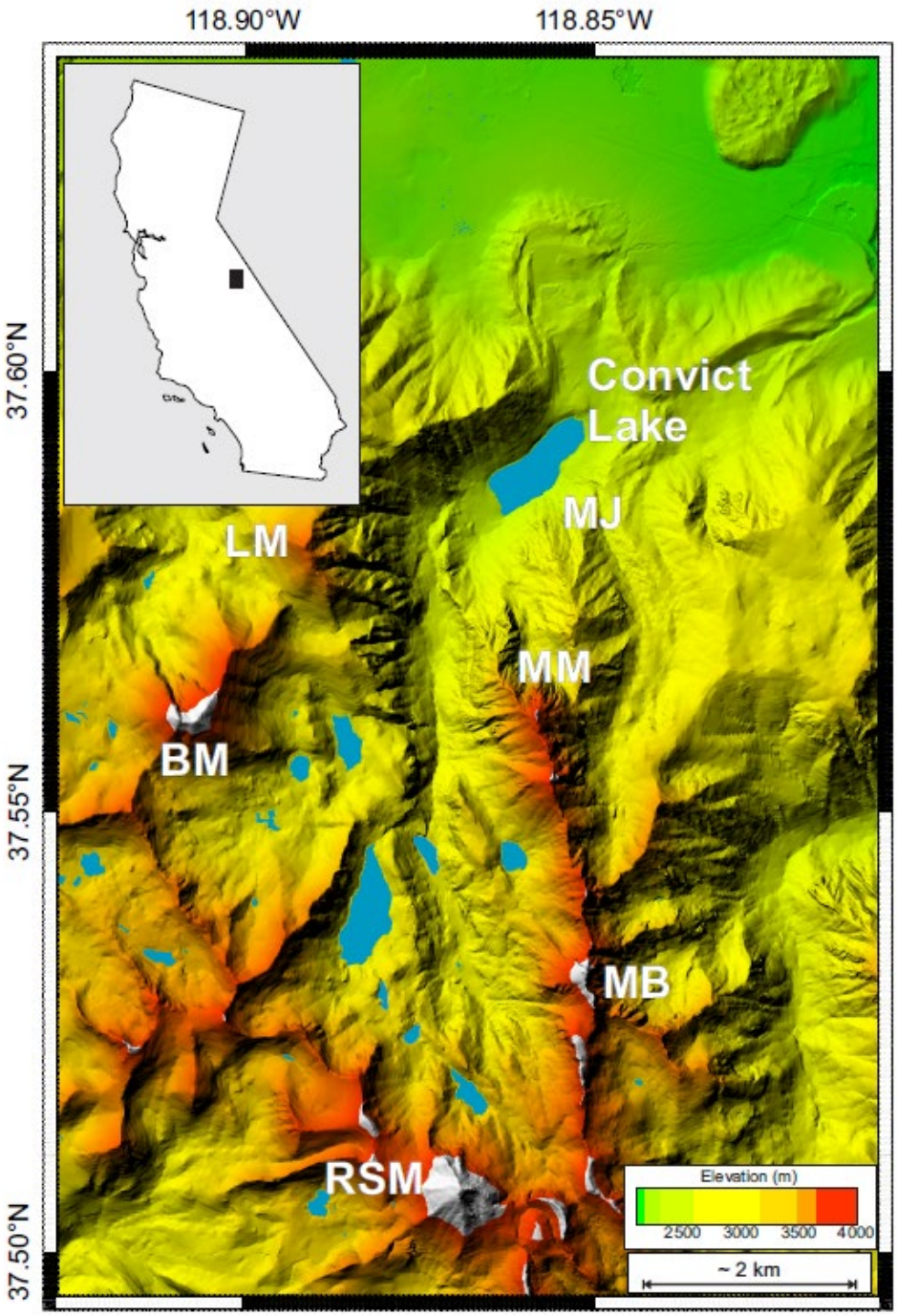

Figure 2. Digital elevation model (1/3 arc second) of the Convict Creek watershed, Eastern Sierras (After McGlue and Woolery, Submitted). Convict Lake lies at the distal end of nine other alpine lakes, all connected via Convict Creek.

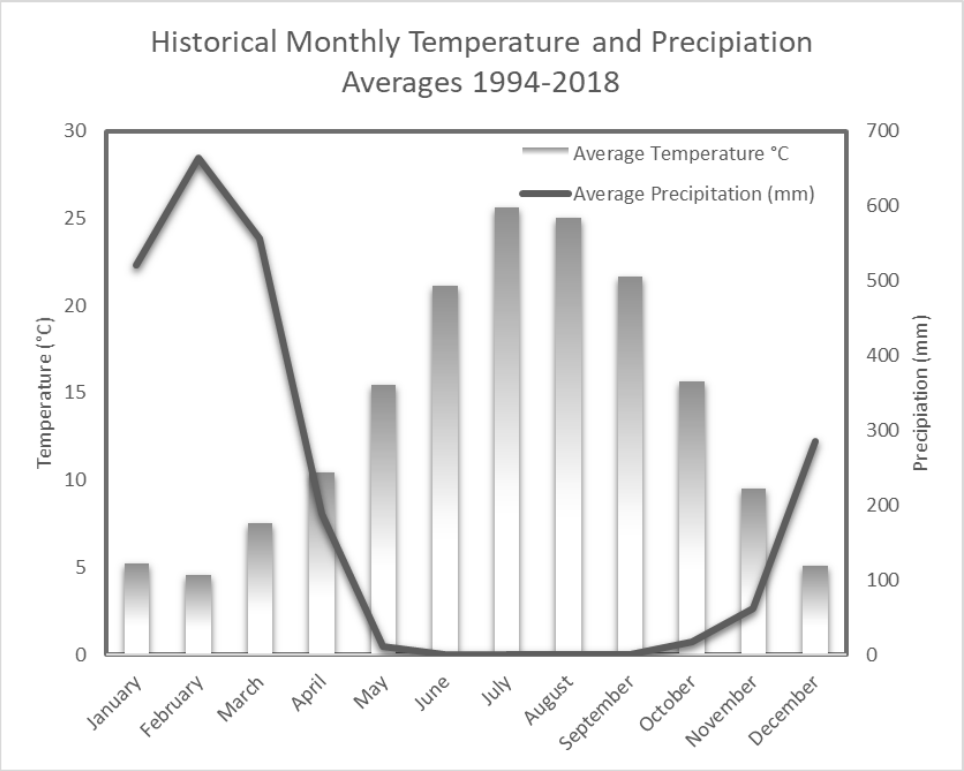

Figure 3. Historical climate data from the Mammoth Lakes ranger station, located less than 1 km east from Convict Lake (NOAA, 2018). Historically, the coolest months of the year are December, January, and February, with daytime highs averaging ~ 5°C. The wettest month of the year is February, with total precipitation averaging ~675 mm since 1994. June through September are the hottest and driest months, with average daily temperatures reaching ~ 25 °C in July, and precipitation averaging <1 mm for all of summer.

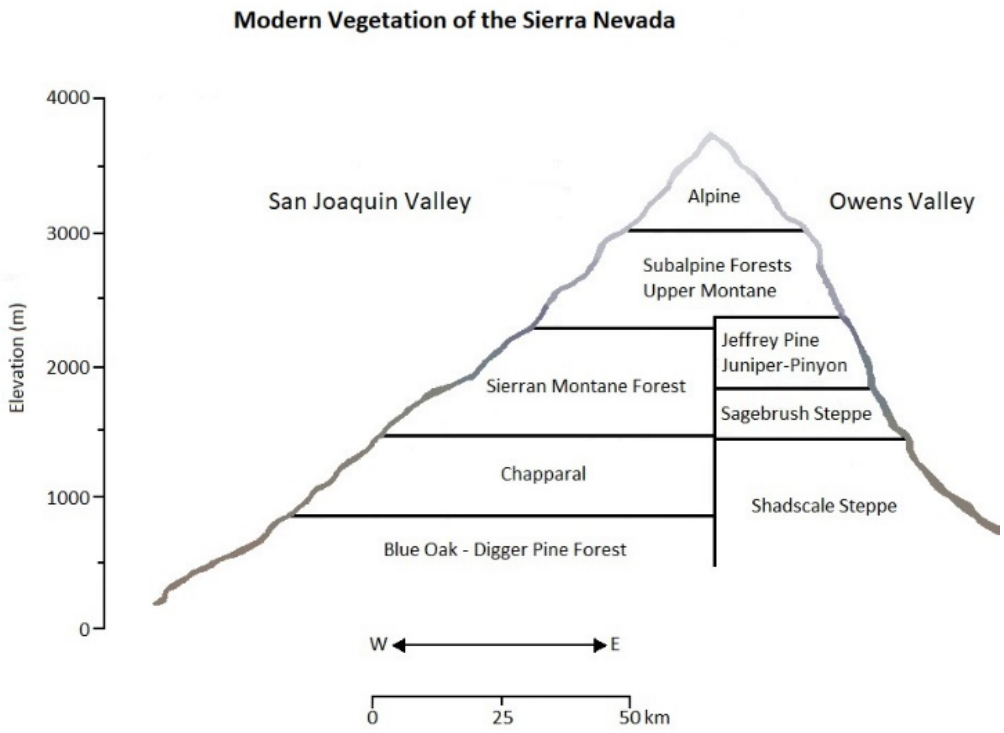

Figure 4. The Sierra Nevada has differing vegetation zones on the western and eastern sides of the crest, after Anderson and Davis (1988). Convict Lake falls within the elevation limits for the upper Montane and Subalpine forest.

2. Methods

To inform the selection of coring locations, Convict Lake was surveyed (~20 km total line length) using an Edgetech 3200 CHIRP acquisition system set at a swept frequency range of 0.5-8.0 kHz (McGlue and Woolery, submitted). The seismic data, paired with a basin-wide lake floor sediment grab sample survey, resulted in a high-resolution bathymetric map for Convict Lake and images of the shallow stratigraphy (McGlue and Woolery, submitted). The best site for coring was determined to be at N 37.58955°, W 118.86892°, with a water depth of ~40.7 m. An UWITEC percussion piston coring platform was used to collect a sequential series of 2-m drives from a primary borehole (CVT-1A-1U) and a secondary borehole (CVT-2B-1U) with staggered starting depths, in order to minimize gaps in the composite vertical stratigraphy created by the piston in the core liner. Multiple surface cores (~ 1-2 m) were also collected using an UWITEC gravity coring system to ensure an intact record of the most recent strata (Table 1). Cores were packaged onsite and shipped to the University of Minnesota's National Lacustrine Core Facility (LacCore) for high resolution imaging, initial core description, GEOTEK multi-sensor core logger (MSCL) physical properties scans, and sub-sampling. The details of the core stratigraphic analysis and radiocarbon age model development will be presented elsewhere (McGlue et al., in prep). Briefly, the overlapping core sections were correlated vertically using magnetic susceptibility data and distinct marker beds, which yielded a ~9.5 m long composite core. The core was ~95% complete with two small gaps, which were produced by coring difficulties encountered in the overlapping drives. The composite core was well preserved and heavy

disturbance of sediments from the coring process was minimal. BACON, an R-based age-depth modeling program that utilizes Bayesian statistics to model sediment accumulation history, was used to produce an age-depth model for the composite core following the methods outlined by Blaauw and Christen (2011). The age model for the composite Convict Lake sediment core contains 12 dated horizons using ^{14}C applied to plant macrofossils and charred plant fragments (table 2) (Figure 5) (McGlue et al., in prep). Macrofossils were abundant in the composite core, and these were used instead of bulk organic material for the radiocarbon chronology, because the source of carbon was conclusively from terrestrial sources. In using bulk organic matter for dating, issues sometimes arise due to the "hard water effect", which is a term for the potential of an old-carbon reservoir within a lake system which comes from dissolved carbonate rocks (Grimm et al., 2009). There is also potential error associated with bulk organic matter dates due to their heterogeneity, with carbon potentially being sourced from older lignite, coal or carbonaceous shales within the watershed (Grimm et al., 2009). Due to the presence of the carbonaceous Mount Aggie and Convict Lake formations, we chose to avoid generating dates on bulk organic matter. All dates were calibrated using the IntCal13 curve within BACON and are expressed as calibrated years before present.

2.1 Pollen Analysis

Pollen samples were collected every 10 cm along the length of the core, resulting in 64 total samples for analysis. Pollen samples were processed using a modified version of the techniques outlined in O'Keefe and Wymer (2017). Approximately 5 g of a 1 cm-wide sediment sample was placed into a 50 mL centrifuge tube with a lycopodium tracer

and topped with a 1% solution of sodium hexametaphosphate. Samples were agitated for 24 hrs and then sieved at 250 μm. The sieved samples were then rinsed with deionized water, centrifuged, and decanted; this processing sequence was repeated until the supernatant fluid appeared clear. A buffered enzymatic solution was prepared for each sample by mixing 0.06 g of cellulase and 0.2 g pectinase in 5 mL of water into 20 mL of sodium citrate solution at a pH of 6.5. Samples then received 25 mL of the enzymatic solution and were agitated for another 24 hours. Samples were rinsed, centrifuged, and decanted three times and then condensed into a 15 mL centrifuge tube. A solution of lithium heteropolytungstate at specific gravity 2.0 was then added to each tube for heavy density separation. After centrifugation, the pollen "float" was pipetted into a clean 15 mL centrifuge tube and rinsed. On the third rinse, the supernatant was discarded, samples were topped with 5 mL of ethyl alcohol and stained with safranin O dye.

A small amount of the pollen separate was pipetted onto a petrographic slide, mixed with a minute amount of glycerin, topped with cover-glass and sealed with clear nail polish. Samples were counted on a Leica Ortholux POL-BK II petrographic microscope to a minimum of 300 grains, with most sample counts exceeding 400 grains. Pollen was identified at 40x magnification. Identifications were confirmed by the morphological descriptions in O'Kapp (2000). Pollen percentages and concentrations were calculated using TiliaIT, a software designed for managing both stratigraphically constrained and unconstrained paleontological data (Grim, 1993). CONISS cluster analysis was completed on the raw data using TiliaIT, from which pollen zones were developed (Figure 6). A ratio of *Artemisia* to Amaranthaceae was also calculated for each pollen sample, following the methods of Mensing et al. (2004) (Figure 7). In that

work, the authors interpreted high (positive) values of this index to represent a wetter climate (e.g., greater *Artemisia*) and negative values represent a drier climate (lower Amaranthaceae); the same interpretive framework was applied in this study. The results are presented as A(*Artemisia)*:C(Amaranthaceae).

2.2 Bulk and Stable Isotope Geochemistry

We developed elemental (total organic carbon, total nitrogen, C:N) and stable isotope geochemical ($\delta^{13}C$, $\delta^{15}N$) datasets on bulk sedimentary organic matter to compliment pollen-based interpretations of paleoenvironments. Samples utilized for the total organic carbon (TOC) and $\delta^{13}C$ analyses were treated with 1 N hydrochloric acid for 1 hr and then rinsed with deionized water until a neutral pH was achieved. Samples utilized for total nitrogen (TN) and $\delta^{15}N$ analysis were not treated with acid, to minimize the potential loss or fractionation of organic nitrogen with acidification (Meyers and Teranes, 2001). Dried sample splits were sent to the University of Utah's SIRFER lab, where they were analyzed using continuous flow isotope ratio mass spectrometry coupled with an elemental analyzed (EA-IRMS). For this analysis, pre-weighed samples in tin capsules were placed into a 1020°C Cr_2O_3 combustion reactor and then moved through the system by oxygen-enriched helium. The capsules ignite, raising the sample temperature to 1800°C and forming H_2O, CO_2 and N_2. Any halogen or sulfur containing gas were chemically removed, and the remaining gasses were sent to a 650°C Cu^+ reducing reactor, where NO_x, CO, and other byproducts of incomplete combustion were reduced and O_2 was removed. Water was then scrubbed from the helium. The final products, N_2 and O_2, were separated on a 3-m Porapak -Q packed gas chromatography

column, before entering the IRMS via an open split interface. Pure reference gasses were tested at specified times to ensure that the machine remains at mass calibration for the entire testing period**.** The standards used include USGS40 and USGS41, and the uncertainty of obtained values was +/- 0.2 ‰.

Table 1. Locations and water depth for all cores used for the composite stratigraphy. CON18-6A-1-1 and CON18-7A-1-1 are short hammer cores, taken to ensure the integrity of the top ~ 3 m of sediment, while CON18-1A-1U and CON18-1B-1U are the offset UWITEC cores that compose a majority of the composite stratigraphy.

Core Name	Lat / Long	Water Depth (m)
(Hammer) CON18-7A-1C-1	N 37.58955°, W 118.85892°	43.1
(Hammer) CON18-6A-1C-1	N 37. 58796° W 118.86018°	42
(UWITEC) CON18-2A-1U-(1-5)	N 37.5917°, W 118.85464°	40.7
(UWITEC) CON18-2B-2U-(1-4)	N 37.59203°, W 118.85468°	40.8

Table 2. Comprehensive list of the materials used to obtain the 12 dates utilized in the BACON derived age model.

Material Dated	**Composite Depth (cm)**	**D^{14}C**	**C^{14} Age**	**Error (+/- years)**	**Sample Size (mg C)**
Macro Plant Fragment	47	-48.4	400	30	0.34
Macro Plant Fragment	102	-86.9	730	30	0.76
Plant - Charcoal Fragment	160.5	-72	600	90	0.03
Plant Macro	209.5	-112.9	960	30	0.27
Plant Macro	280	-196.7	1760	30	0.48
Plant Macro	317.5	-322.6	3130	30	0.37
Plant Macro	335	-303.5	2905	30	0.93
Plant Macro	406	-413.5	4285	30	1.08
Plant Macro	494.5	-447.5	4765	30	1.02
Plant Macro	519.5	-541.5	6260	60	0.12
Plant Macro	614.5	-645.8	8340	35	1.18

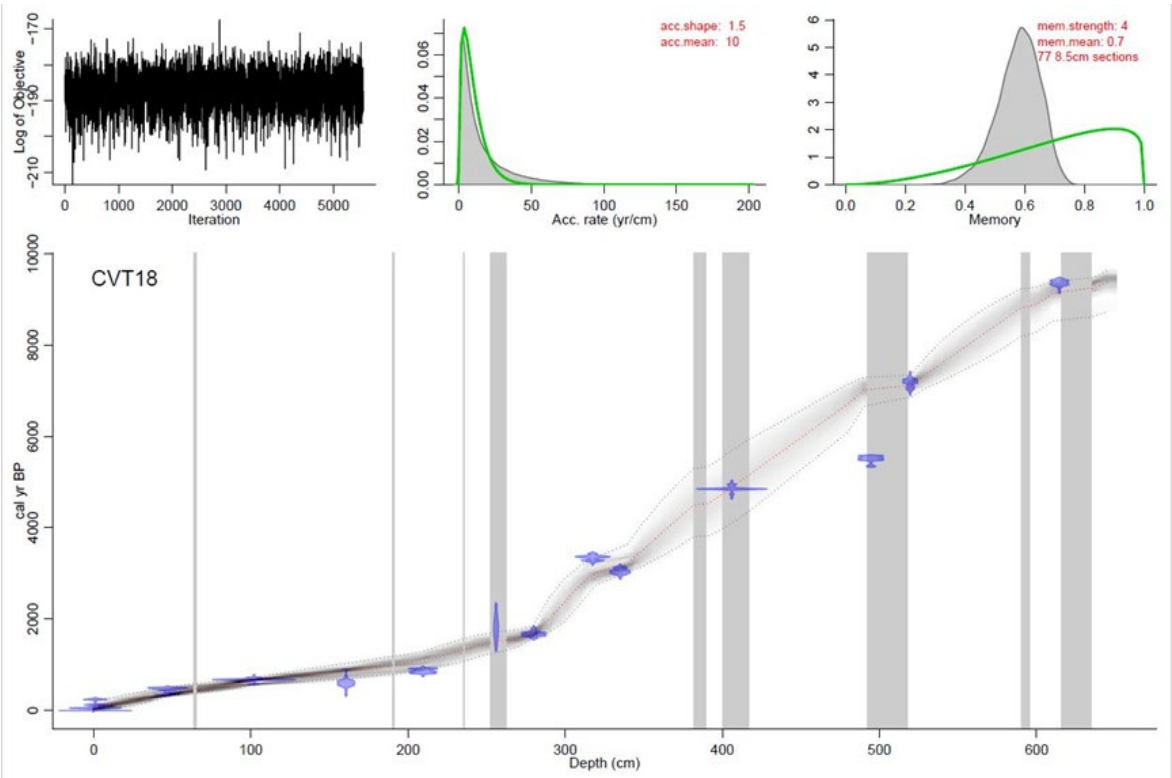

Figure 5. BACON, an R-based age-depth modeling program that utilizes Bayesian statistics to model sediment accumulation history, was used to produce an age-depth model for the composite core. The age model for the composite Convict Lake sediment core contains 12 dated horizons using ^{14}C applied to plant macrofossils and charred plant fragments.

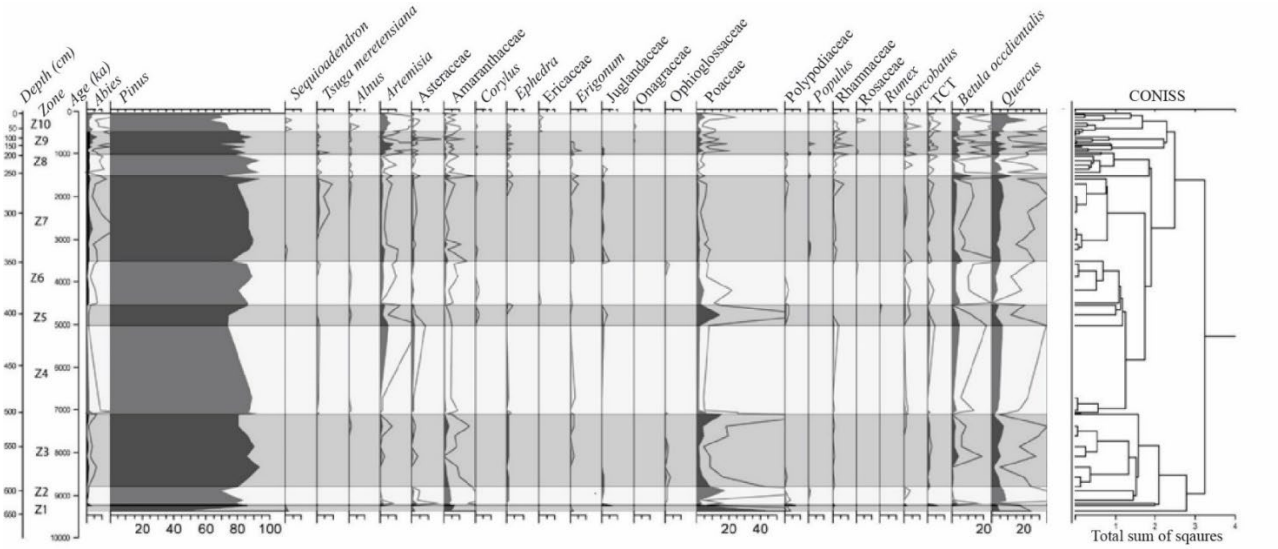

Figure 6. There are 10 distinct pollen zones in the vegetation record that were determined using CONISS cluster analysis in TiliaIT (Grim, 1987; www.tiliait.com). Gray and white bands are used to aid in the visualization of the calculated zones.

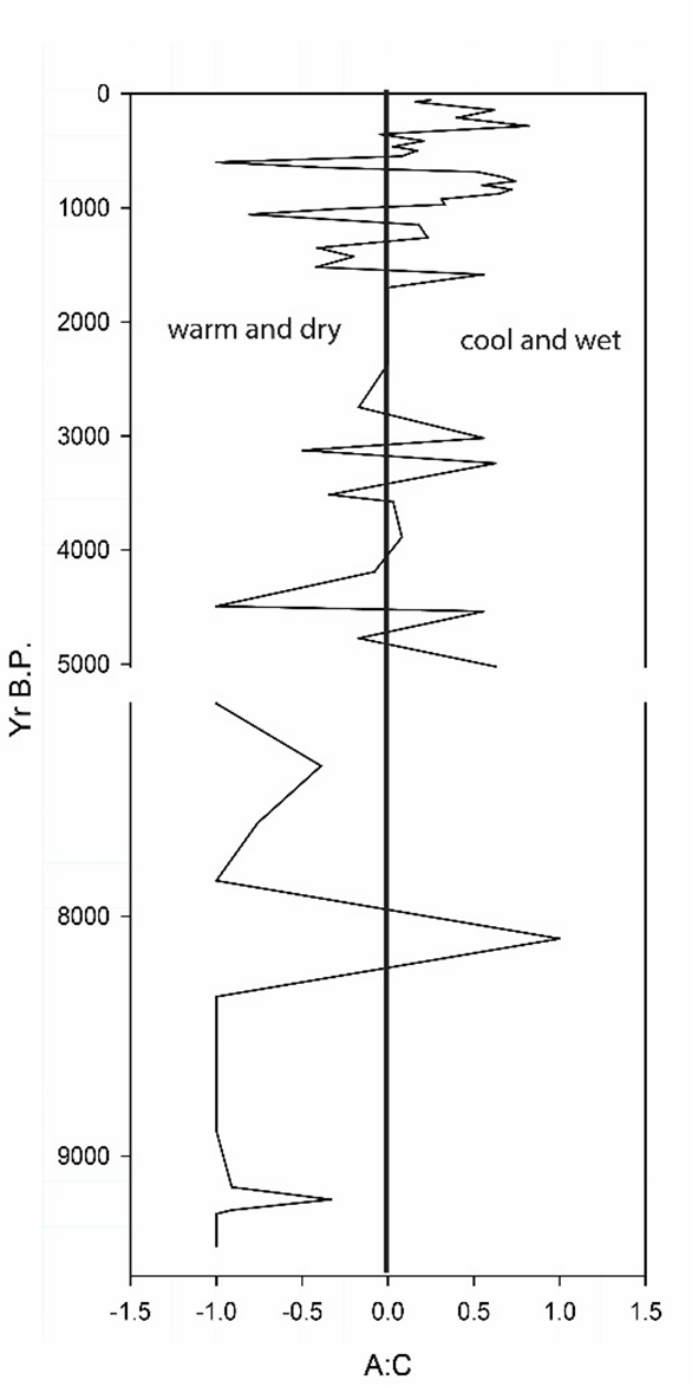

Figure 7. A ratio of *Artemisia* to Amaranthaceae (A:C) was calculated following the methods of Mensing et al. (2004). These values were calculated using an equation of a-(c+s)/(a+c) where a = *Artemisia*, c = Amaranthaceae, and s = *Sarcobatus*. Positive values are interpreted to represent a cool and wet paleoclimate whereas negative values are considered to represent a warm and dry paleoclimate (Mensing et al., 2004).

3. Results

Pollen zonation was based on CONISS cluster analysis (Grimm, 1987). Pollen presence is discussed using percentages of the total taxa counted. In Figure 6, an exaggeration of 5x of the reported percentages was used to aid in visualizing the changes in less common taxa, as the record is dominated by *Pinus*, with values ranging from 65-90% in all counted samples. Pollen concentrations were excellent, with an average of 48,599 grains/g. Pollen preservation was fair to good (Figure 8); unidentifiable grains account for 2% or less of all samples.

Zone 1

Pollen zone 1 shows the post glacial establishment of vegetation from 9,380 to 9,240 yr B.P.. The zone is dominated by ~85% *Pinus* and other taxa that exceed 1% pollen abundances are limited to Amaranthaceae and Poaceae. The A:C value is -1 for the entirety of this interval.

Zone 2

Pollen zone 2 (9,240–8,890 yr B.P.) exhibits an initial increase in pollen abundances of herbaceous taxa *Artemisia* and Asteraceae as well as *Betula occidentalis* from the base of the zone to ~9,130 yr B.P.. Abundances of these taxa gradually decrease moving up section, whereas abundances of Amaranthaceae, *Sarcobatus* and Poaceae increase from 9,130 – 8,890 yr B.P.. The A:C ratio for this interval ranges from -1 to -0.3. The least negative A:C value in this zone coincides with the highest percentage of *Betula occidentalis* (Figure 6).

Zone 3

Pollen zone 3 (8,880 - 7,110 yr B.P.) is dominated by *Pinus*, with percentages consistently > 79%, whereas other important pollen taxa include *Quercus*, Poaceae, and Amaranthaceae. *Artemisia* exceeds ~1 % at 7,370 yr B.P., and *Betulaceae occidentalis* is >1% from 8,090 - 7,370 k yr B.P.. Near the top of this zone (7,610 – 7,370 yr B.P.), there is a significant increase in pollen abundances of Poaceae from 3.7% to 15.3%, and a decrease in *Quercus* from 6.9% to 1.0%. The A:C value for this interval is mostly -1, but it increases slightly from 7,610 – 7,360 yr B.P..

Zone 4

In pollen zone 4 (7,110 - 5,020 yr B.P.), it is important to note that there is a sampling gap from a depth of 480 cm (6,700 yr B.P.) to 411.5 cm (5,020 yr B.P.); this portion of section is missing due a lack of overlap section in the primary and secondary boreholes. From ~7,100 - 6,700 yr B.P., *Pinus* percentages are > 85% and other important taxa include *Abies,* Poaceae, and *Quercus* (Figure 6). *Betula occidentalis*, Amaranthaceae, and *Sarcobatus* are also consistently present during this interval. At 5,020 yr B.P., there is a significant increase in herbaceous taxa like *Artemisia* (4.9%), Asteraceae (1.6%) and Amaranthaceae (1.1%). The riparian taxa *Betula occidentalis* is present at abundances of 4.4% and *Quercus* abundances are on average 6.8% during this interval. Other trees and shrubs present include *Abies,* Rhamnaceae, and TCT types. At the beginning of this zone, the A:C is -1, and the curve trends towards positive values moving up section. A positive A:C is reached for the first time in the record at 5,020 yr B.P..

Zone 5

Pollen zone 5 (5,020 – 4,490 yr B.P.) represents a period of enhanced high abundances of herbaceous taxa. Total herbaceous taxa percentages are consistently above 4%, with an average of 9.3% for the duration of this zone. Betulaceae is consistently present above 1% with an exception at 4,540 yr B.P., where there were no *Betula occidentalis* or *Corylus* grains present. *Quercus* exceeds 2.5% nearly throughout the zone, with an exception at 4,490 yr B.P., where no *Quercus* grains were encountered. The A:C for this interval ranges from -1.0 – 0.5.

Zone 6

Pollen zone 6 (4,490 – 3,510 yr B.P.) is dominated by tree and shrub taxa. *Pinus* is consistently > 75%, whereas *Abies* is continuously > 0.5%. Juglandaceae reaches 1% at 3,510 yr B.P., near the top of the zone. Herbaceous taxa are present and relatively stable in this zone, with *Artemisia* > 1%, and *Amaranthaceae* is > 0.7% on average. Other important taxa include *Betula occidentalis* and *Quercus*, which are both > 2%. The A:C for this interval ranges from -1.0 to 0.03.

Zone 7

In pollen zone 7 (3,510– 1,580 yr B.P.), tree and shrub taxa dominate total pollen percentages, with *Pinus* (> 78%) and *Abies* (> 0.8%) having particularly high abundances on average. Average *Betulaceae occidentalis* is > 0.5%, whereas *Quercus* is > 3%. The percentages of the important herbaceous taxa are low and at times variable for this zone, with *Artemisia* at > 1% at 1,990 – 1,700 yr B.P., and Amaranthaceae reaching above 1% by ~1,700 yr B.P.. There is a significant amount of variability in the A:C for this zone, and values range from -0.5 – 0.5.

Zone 8

Pollen zone 8 (1,580 – 1,150 yr B.P.) is highly variable, with pollen abundances of only *Pinus* and *Quercus* consistently remaining around >1%. At 1,580 yr B.P., the important taxa include *Abies, Pinus, Quercus*, and a very small amount of the indicator species *Tsuga mertensiana* is present. At 1,520 yr B.P., *Betulaceae occidentalis* abundances reach the high values of the record (11.5%), and other important taxa include *Abies, Artemisia, Asteraceae*, Amaranthaceae, *Erigonum*, Poaceae, and *Querc*us. The A:C for this interval is variable, ranging from -0.4 – 0.5.

Zone 9

Pollen zone 9 (1,150 - 690 yr B.P.) is an interval of high amplitude variability in the Convict Lake palynological record. *Betulaceae occidentalis* abundances are consistently > 2%. *Artemisia* percentages steadily increase moving up through this zone, with a low of 0.2% at 1,010 yr B.P. and a high of 8.1% at 770 yr B.P., followed by a decrease to 2.5% from 730 to 690 yr B.P.. Amaranthaceae percentages are variable but > 1% at 1,060, 1,010, 920, 880, 800, and 760 yr B.P.. Poaceae percentages are variable but > 1% from 920 to 690 yr B.P.. *Abies* is an important taxon for the entire interval except at 920 yr B.P.. *Pinus* percentages range from a high of 92% at 1,150 yr B.P. to a low of 63% at 770 yr B.P.. The A:C ranges from -0.8 – 0.7, however most of the zone remains positive; the two negative values occur from 1,060 – 1,010 yr B.P..

Zone 10

Pollen zone 10 (690 yr B.P. – present) is highly variable. While *Pinus* percentages dominate total pollen counts and range from 60-83%, herbaceous and riparian taxa have

high abundances during this interval as well. *Betulaceae occidentalis* is consistently >1% except from 650 - 600 yr B.P., where it decreases to 0.7%. *Quercus* is present at percentages above 2%. *Artemisia* is >1%, with an exception at 600 yr B.P., where there were zero *Artemisia* grains. Amaranthaceae has a less consistent presence and is only considered an important taxon at 650 yr B.P., from 550 – 360 yr B.P., 210 yr B.P., and at 70 yr B.P.. Poaceae is an important taxon for the entirety of this interval with exceptions at 550 yr B.P., and from 360 - 280 yr B.P.. The A:C values are also variable and range from -1.0 to 0.6, but are mostly positive. Negative A:C occurs from 650 – 600 yr B.P., and again at 350 yr B.P..

3.1 Detrended Correspondence Analysis

A detrended correspondence analysis was completed on the pollen data to determine the presence of environmental controls on vegetation response (Oksanen et al., 2019) (Figure 9). Axis 1 has an eigenvalue of 0.2193 and an axis length of 2.4478 standard deviations. Axis 2 has an eigenvalue of 0.167 and an axis length of 2.0806 standard deviations. When using a detrended correspondence analysis on an ecological dataset, the first axis provides a metric of species turnover amongst samples along that axis, and four standard deviations indicates a complete turnover of species composition (Ivory et al., 2018; ter Braak 1985).

Mensing et al. (2004) demonstrated that the replacement of *Artemisia* with Amaranthaceae (formerly Chenopodiaceae) occurred during especially arid intervals in the Great Basin throughout the Holocene. Further, Gillespie and Loik (2004) demonstrated that *Artemisia tridentata* seedlings use an increase in water availability efficiently, and a sudden increase in water increases their rate of stomatal conductance

and transpiration. It is important to note that this study was completed at the Sierra Nevada Aquatic Research Laboratory, located in Mammoth Lakes, California and that *Artemisia tridentata* is the same species that currently grows in the Convict Lake watershed. These observations support the notion that in times of increased precipitation, *Artemisia* could effectively spread and increase sagebrush canopy cover. In Figure 9, Amaranthaceae falls directly above -1 on axis 1 and *Artemisia* falls directly above 1 on axis 1 of the DCA. This indicates that axis 1 represents a gradient of understory vegetation response to precipitation.

Poaceae and Polypodiaceae are present in the same quadrant as Amaranthaceae, which further supports the interpretation of a drier, more open understory in samples that fall on this section of axis 1. *Betula occidentalis* and *Artemisia* are present within the same quadrant, *Betula occidentalis* being a riparian taxon that is extremely water dependent (Junak et al., 2007), which supports the idea that samples that fall on this section of axis 1 are representative of wetter climatic conditions.

3.2 Chemostratigraphic Results

There are three prominent chemostratigraphc units within the record (Figure 10). The units span from ~ 9,400 – 6,700 yr B.P. (unit I), ~ 5,020 – 2,000 yr B.P. (unit II), and ~ 2,000 yr B.P. – present (unit III), respectively. These units also fall closely within the stratigraphic bounds of the three seismic units documented by McGlue and Woolery (submitted).

Unit I is characterized by low average TOC and TN, at 1.6 and 0.1 wt %, respectively. The C:N values are relatively high in unit I, with an average of 15.2. $\delta^{13}C_{org}$

values are low to moderate and average -23.3 ‰, whereas the $\delta^{15}N_{org}$ values average 3.3 ‰, which is on par with the data from the overlying units. There are three anomalous events in which values noticeably diverge from the average trend: at 9,130 yr B.P., 7,370 yr B.P. and 6,710 yr B.P. (Figure 10). These events are all similar in nature, with enriched $\delta^{13}C_{org}$ values, very low TN, and relatively high TOC and C:N. Aside from these anomalous events, there is a lack of a long-term trend in this unit.

In unit II, TOC and TN average 2.7 and 0.3 wt. %, respectively. The TOC shows the most variability within the unit, and trends toward higher values moving toward the upper contact (Figure 10). The C:N decreases overall in unit II, with an average value of 10.3. The average $\delta^{13}C_{org}$ is -25.8 ‰, whereas the average $\delta^{15}N_{org}$ is ~3.4 ‰; both stable isotope curves are relatively invariant over most of the unit. The elemental geochemistry of unit II is relatively stable, with only one truly anomalous event at ~ 4,860 yr B.P., which is characterized by a spike in $\delta^{13}C_{org,}$ very low TOC and TN, and a relatively high C:N value.

Unit III exhibits the highest variability in the geochemical data (Figure 10). The TOC and TN reach their highest average values in the core, at 3.4 and 0.3 wt % respectively. The average C:N is 12.5, whereas the $\delta^{13}C_{org}$ values range from -9.9 ‰ to -28.0 ‰ and average -25.0 ‰. The $\delta^{15}N_{org}$ values are quite variable, ranging from 0.6 – 5.9 ‰, and the average value is 3.4 ‰. Overall, $\delta^{15}N_{org}$ decreases moving up section, whereas TOC generally increases upward toward the top of the unit. There are several high amplitude shifts in the geochemistry of unit III that are characterized by depleted $\delta^{13}C_{org}$ and a significant increase in C:N. Events of this kind are observed at ~ 1,490, 1,190, 1,030, ~650, and ~ 177 yr B.P.. There is one anomalous event at ~ 550 yr B.P.

that is marked by a different signal, where $\delta^{13}C_{org}$ is enriched at -28.3 ‰, and the C:N is measured at 8.9.

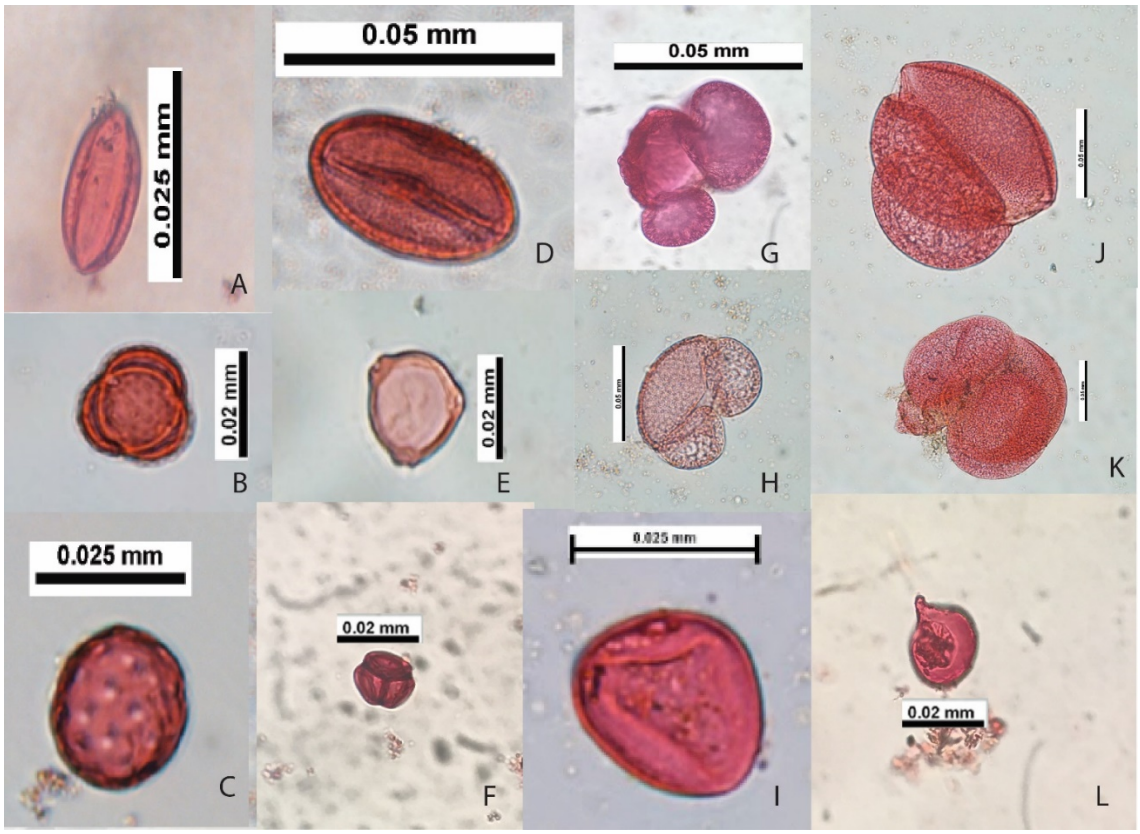

Figure 8. Pollen preservation was fair to good; pollen types shown here are the most discussed for this study. A.) *Ephedra*, B.) *Artemisia*, C.) Amaranthaceae D.) *Erigonum* E.) *Betula occidentalis* F.) Ericaceae G.) *Tsuga meretensiana* H.) *Pinus* I.) Poaceae J.) *Abies* K.) *Abies* L.) *Seqouiadendron giganteum*

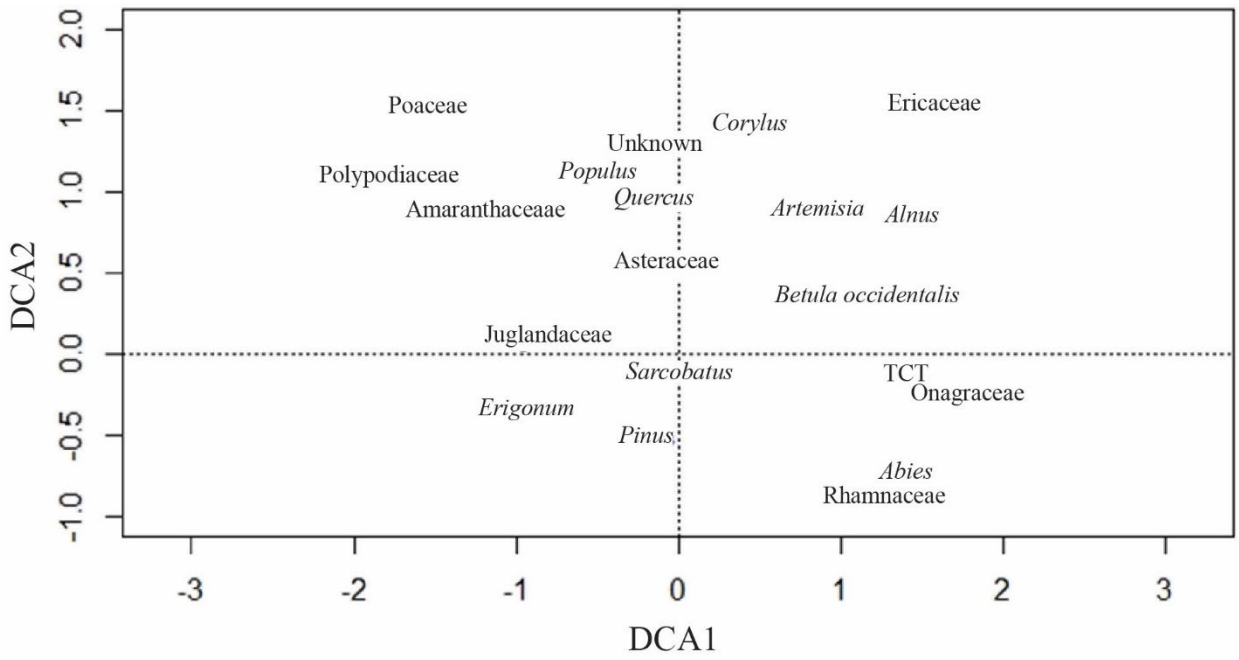

Figure 9. A detrended correspondence analysis was completed on the pollen data to determine the presence of environmental controls on vegetation response. When using a detrended correspondence analysis on an ecological data set, the first axis provides a metric of species turnover amongst samples along that axis, and four standard deviations indicates a complete turnover of species composition (Ivory et al., 2018; ter Braak 1985).

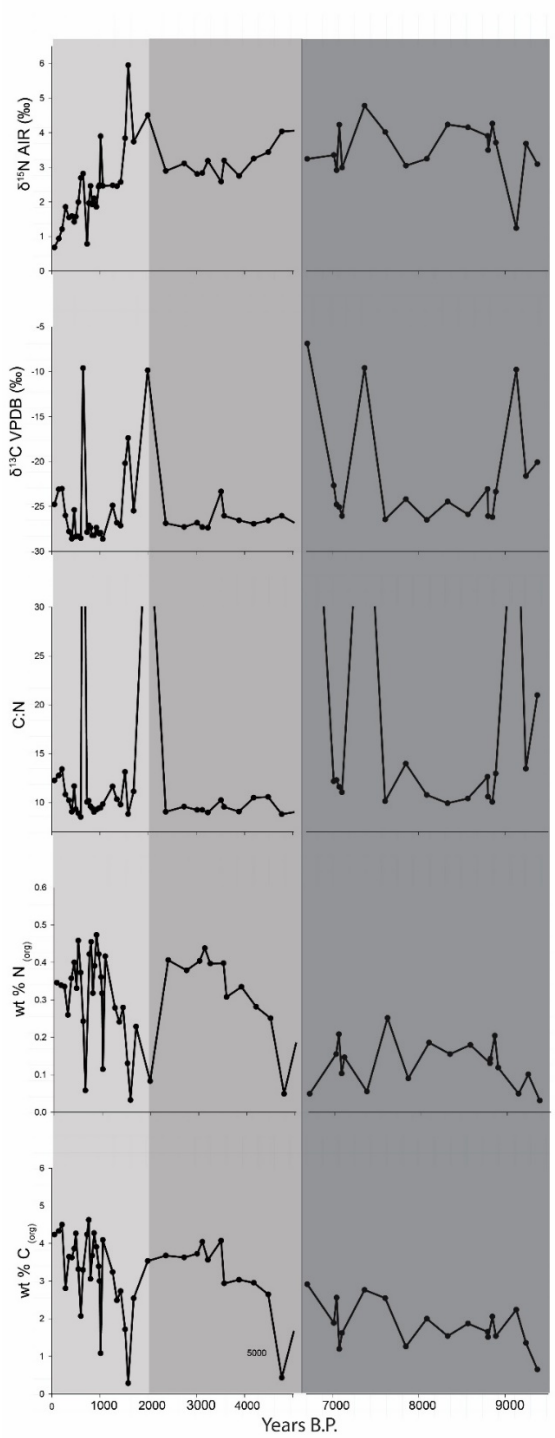

Figure 10. Elemental and organic stable isotope analysis of lake sediments revealed three distinct chemostratigraphic units that align with seismic stratigraphic units discovered by McGlue and Woolery (in review). Grayscale banding is used to aid in the visualization of these three units.

4. Discussion

4.1 Use and Implications of Pollen and Geochemical Data

Pollen based paleo-vegetation records provide insight on regional forest ecology shifts through time and the relationship these changes have to temperature and precipitation, which in northeastern California commonly links to the dynamics of winter snowfall (Assarsson and Granlund, 1924; Jansonius and McGregor, 1996). To supplement the pollen record at Convict Lake, organic matter geochemistry, including stable isotopes of carbon and nitrogen were pursued on bulk sedimentary organic matter (OM). In any limnological environment, stable isotopes, specifically $\delta^{13}C_{org}$ and $\delta^{15}N_{org,}$ as well as C/N, may vary in response to rates of primary production, phytoplankton composition, organic matter degradation, bacterial growth in the water column and sediment, biosynthesis, and input from allochthonous organic sources (e.g., Brenner et al., 1999, Meyers and Teranes, 2003, Gasiorowski and Sienkiewicz, 2013). The primary sources of sedimentary OM from which stable isotope data is derived comes from: (1) non-vascular aquatic plants (phytoplankton) that contain very little cellulose and lignin, but is enriched in nitrogenous materials like proteins and amino acids, and (2) vascular plant matter that contains carbon-rich tissues from macrophytes, trees, grasses, and shrubs from the surrounding watershed (Meyers and Teranes, 2003). The carbon in bulk OM derived from either plankton or higher plants retains its unique isotopic signature, therefore allowing inferences of lake trophic level and influences of drainage basin vegetation on a lake system (Meyers and Teranes, 2003). It should be noted that in a hydrologically open basin like Convict Lake, organic richness as inferred by TOC values can be linked to a host of conditions, including high primary productivity, advection of

terrestrial OM to the sediment pile, good (modest) preservation potential when water levels are high (low), and variable dilution; these controls have been observed to influence over-filled lakes throughout geological history (Bohacs et al., 2000).

$\delta^{13}C_{org}$ values for C_3 plants and algae are typically between -30 and -22‰, whereas the global average for C_3 plants is approximately -28.5 ‰ (Kohn, 2010; Vreca and Muri, 2010). While the $\delta^{13}C_{org}$ signature cannot distinguish among OM input from various phytoplankton versus terrestrial C_3 plants, it can aid in inferring the presence of C_4 plants growing within the watershed, which average -15 to -10 ‰ (Gasiorowski and Sienkiewicz, 2013). Typical $\delta^{15}N_{org}$ values average ~ 1.0 ‰ for C_3 land plans, while the range of values for phytoplankton that assimilate nitrate is ~ 2.0 – 14.0 ‰. In contrast, cyanobacteria that fix N_2 generally exhibit $\delta^{15}N_{org}$ below ~2.0 ‰ (Talbot and Johannessen, 1992). It is important to note that water column stratification can limit internal nitrogen cycling in lake systems, which can affect phytoplankton competition by constraining the availability of different types of DIN available to the photic zone.

The C:N for most aquatic plants and phytoplankton is below 10, whereas higher values may indicate the presence of both aquatic and terrestrial OM (Mackie et al., 2005, Zong et al., 2006, Gasiorowski and Sienkiewicz, 2013; McGlue et al., 2015). The C:N signature for lacustrine OM dominated by terrestrial vegetation is often above 20-30 (Meyers and Ishiwitari, 1993). These reference points allow for the broad inference of vegetation types present at the time of OM deposition, assuming the sediments have not undergone extensive diagenesis resulting in the preferential loss of labile nitrogen.

Higher $\delta^{13}C_{org}$ values can signal higher rates of photosynthesis when CO_2 is abundant in the water column and key nutrients (N, P) are not limited (Meyers and

Ishiwitari, 1993, Cohen, 2003). Thus, increases or decreases in the carbon isotopic signature of sedimentary OM can be used to infer changes in paleoproduction. Interpretations of paleoproduction therefore rely on low C:N values, which provide confidence in an algal provenance for the OM. When CO_2 is limited and lake water pH is high, certain algae can switch over to HCO_3^- for photosynthesis, which leads to more enriched (as high as 9‰) carbon isotopic composition in sediments (Meyers and Terranes, 2001).

In dimictic lakes like Convict Lake, fractionation of nitrogen accompanies the high productivity that occurs as nutrients are reintroduced to epilimnion during spring and early summer, which leads to an increase in $\delta\,^{15}N_{org}$ (Cohen, 2003; McFadden et al., 2004). Overall, enrichment of $\delta\,^{15}N_{org}$ that coincides with other productivity indicators (e.g., TOC), can be used as an indicator of increased paleoproductivity (Cohen, 2003).

4.2 Early Holocene (Zones 1-3, 9,380 - 8,800 yr B.P.)

In the Convict Lake pollen record, useful pollen and stable isotope data were not produced until a composite depth 645 cm (~9,380 yr B.P.), where there is abundant *Pinus,* Poaceae, Amaranthaceae and *Quercus*, with an A:C that is persistently -1. We interpret this pollen assemblage to represent the initial colonization of the landscape after glacial retreat, and a montane chaparral forest with an open understory was present. This vegetation assemblage is mostly likely indicative of poor soils surrounding the basin due to the retreat of the Convict glacier. We interpret that the climate was warmer and drier during this interval than what is observed in the present, allowing for rapid expansion of

Poaceae, which reaches maximum pollen abundances of 20% during this interval (Figure 6). This interpretation is consistent with the negative A:C.

The paleoenvironmental data from Mono Lake vary for the early Holocene. Paleoshoreline data presented in Ali (2018) suggests several cycles of lake level change between 1975-1950 m a.s.l., whereas shallow water sediment cores suggest a relatively wet climate on the basis of minimal carbonate content (Zimmerman et al., in rev). Deepwater sediments discussed in Hodelka et al. (in rev) provide evidence that Mono Lake was relatively deep and had anoxic bottom waters during the early Holocene; this interpretation is in accord with those of Newton (1994), who suggested that the lake was meromictic at that time. The early Holocene sediments (~10.9-8.7 kyr B.P.) observed by Hodelka et al. (in rev) contain finely laminated muds that lack any evidence of bioturbation, and generally exhibit very low magnetic susceptibility, which is broadly consistent with the low carbonate content observed in the early Holocene sediments of Zimmerman et al. (in rev). From a geochemical perspective, the early Holocene was characterized by low C:N values and high $\delta^{13}C_{ORG}$ and TOC in Hodelka et al. (in rev), and those values were interpreted as a signal of high productivity in a relatively deep lake.

The water supplying Mono Lake during early Holocene highstands was probably sourced from retreating glaciers and heavy winter snowfall in the adjacent Sierras. In contrast to Mono Lake, data from the present study suggests that the Convict Creek watershed was drier at ~8,800 yr B.P.. Taxa indicative of drier conditions, specifically Amaranthaceae and Poaceae, make up 21% of total pollen assemblage at 8,800 yr B.P., while *Pinus* represents 68.5% of total pollen assemblage. This *Pinus* percentage is very

low considering the whole-core averages for Convict Lake (Figure 6), and lowstands are marked by decreases in *Pinus* at Mono Lake (Davis, 1999). Overall, decreases in *Pinus* coincide with more negative A:C values in this study, which supports the idea that during periods of aridity, *Pinus* populations decline (Figure 11). Davis (1999) also observes a lowstand at Mono Lake at 8,800 yr B.P., which is marked by the presence of thin sand layer and relatively low abundances of *Pinus*. In Hodelka et al. (in rev), there is a change in sedimentation at Mono Lake ~8,700 yr. B.P., which is marked by a transition from finely laminated lake mud with sharp contacts to thicker laminations with diffuse contacts and the first observation of coarse-grained laminations in the record, which implies a shallowing of Mono Lake. We interpret the Convict Lake data, contextualized by the observations of Davis (1999), Zimmerman et al. (in rev) and Hodelka et al. (in rev), to represent a lowstand that occurred at Convict Lake beginning at ~ 8,800 yr B.P. It is important to note that at this time, Convict Lake was still in its infancy following the last deglaciation (McGlue and Woolery, submitted).

In the earliest Holocene chemostratigraphy, TOC and TN are very low, whereas $\delta^{13}C_{org}$ and $\delta^{15}N_{org}$ are relatively enriched (Figure 10). C:N values are quite high, which we interpret to reflect a strong influence of terrestrial carbon on the OM pool and dilution of the lake. This aspect of the geochemical record is consistent with the pollen, as a lowstand Convict Lake might be susceptible to a greater flux of terrestrial OM, and the elevated $\delta^{13}C_{org}$ are consistent with a contribution of C_4 grasses. Progressing towards the end of the early Holocene (~9,200 - 8,800 yr B.P.), TOC begins to increase and C:N starts to decrease, whereas $\delta^{13}C_{org}$ and $\delta^{15}N_{org}$ remain enriched. The $\delta^{15}N_{org}$ values at this time are suggestive of nitrate assimilation, and diatoms observed on smear slides are

consistent with a lake environment conducive to periodic mixing that recharged the DIN pool. Importantly, the lower C:N values are consistent with a shift from terrestrial to algal dominated organic matter. A deeper lake occupying lower Convict Creek valley at this time is consistent with the declining C:N and greater OM burial, which together suggest higher algal production and a lake floor environment more conducive to OM preservation. Thus it is likely that the lake was relatively low throughout the Early Holocene and was just starting to transgress during the transition to the Middle Holocene.

4.3 Middle Holocene (Zones 3-5, 8,800 to 4,490 kyr B.P.)

The mid-Holocene is a relatively stable period in the Convict Lake record based on both pollen and geochemical data, similar to other Sierran pollen records (Anderson and Davis, 1988, Anderson, 1990, Davis, 1999). *Pinus*, Amaranthaceae, Poaceae and Quercus dominate the vegetation record, as well as *Betula occidentalis*, *Abies*, and other T-C-T types; these data indicate Convict Lake was transgressing at this time. We interpret the pollen assemblage to reflect a climate transition toward cooler and wetter conditions, for TCT types become more common, as do riparian taxa such as *Betula occidentalis*. It is also likely that the consistent presence of *Betula occidentalis* marks the establishment of Convict Creek as an axial drainage entering into Convict Lake, as these plants are associated with high edaphic moisture, such as along riverine corridors (Smith et al., 1995).

From 7,610 - 7,370 yr B.P., the A:C steadily increases from -0.8 to -0.4, which we interpret as increasing precipitation for this period. At the same time, there is an increase in *Quercus*, Poaceae, and other Asteraceae types, and the first appearance of *Alnus*.

Geochemically, C:N remain in the range of 9 – 11 and $\delta^{13}C_{org}$ values remain within the threshold limits for C_3 plants, while TOC and $\delta^{15}N_{org}$ increase. We interpret these values to indicate that chiefly algal biomass contributed to the provenance of the OM. Zimmerman et al. (in rev) inferred a brief deepening of Mono Lake between 7,610 and 7,200 yr B.P. on the basis of a decrease in both Ca/Ti and aragonite flakes in shallow water sediments. This deepening of Mono Lake co-occurs with the observed increase in precipitation at Convict Lake, thus we suggest an increase in regional precipitation between 7,610 and 7,370 yr B.P.

By ~7,110 yr B.P., the A:C attains a value of -1.0 and maintains that value until ~6,710 yr B.P. Poaceae percentages reach maximum values at this time, ranging from 1-15 % for the interval. Negative A:C and high percentages of Poaceae lead us to interpret a transition to a warm and dry paleoclimate for this interval. TOC is moderate – low for this interval, and C:N ratios as well as $\delta^{13}C_{org}$ values indicate an algal provenance for OM. It is likely that warm and dry conditions lead to an earlier spring melt as well as a shallower Convict Lake, which would allow for moderate – high production, due to a prolonged period of mixing. The low TOC values can likely be explained by a decrease in anoxia that resulted from a shallowing of the lake. Inferred warm and dry paleoclimate for this time period is recorded in numerous regional records, including from Mono Lake (Zimmerman et al., in rev), Tulare Lake in the Sierra Nevada (Negrini et at., 2006; Blunt and Negrini, 2007), Owens Lake (Bacon et al., 2006), and in Lower Bear and Silver Lakes in the Mojave (Kirby et al., 2012; Kirby et al., 2015).

Following the gap at ~6,710 – 5,020 yr B.P., the A:C reaches a positive value of 0.6, which is the beginning of pollen zone 5 and marks the first point in the Convict Lake

record in which there is more Artemisia present than Amaranthaceae and *Sarcobatus*. Other important taxa in this time interval include Asteraceae and the riparian taxa *Betula occidentalis*. It is important to note that *Tsuga mertensiana* was identified in this interval and it is an indicator species of subalpine forest (Anderson and Davis, 1988). *Tsuga mertensiana* is present in this interval at 0.3%, which we interpret as evidence of subalpine forest at higher elevations within the Convict Creek drainage basin. The geochemical signal indicates that at this time of wetter a climate, as OM is dominated by algae, with $\delta^{13}C_{org,}$ $\delta^{15}N_{org}$ and C:N values being -26.5 ‰, 4.0 ‰ and 10, respectively. Primary productivity for this period is inferred as being high, for $\delta^{15}N_{org}$ and TOC values are relatively high in comparison to the rest of the record (Brenner et al., 1999; Meyers and Terranes, 2001; Cohen, 2003). We interpret that lake level was high at Convict Lake during this period, driven by more winter precipitation and colder temperatures, which would serve to reduce water loss by evaporation and maintain ice cover longer into the spring, delaying the onset of summer stratification. A colder, deeper lake is favorable for strong water column mixing in the late spring, providing the nutrients needed for higher primary productivity and amenable to higher TOC (Poschke et al., 2015).

From 5,000 – 4,490 yr B.P., the vegetation is variable. At 4,770 yr B.P., the A:C is -0.2, and Poaceae abundances are very high at 14%, indicating a warm and dry climate. $\delta^{13}C_{org}$ is -26.3 ‰, while $\delta^{15}N_{org}$ and C:N values are 4 and 10, respectively. This indicates that primary productivity is relatively high, and $\delta^{13}C_{org}$ is likely reflective of the DIC pool in the water column and its drawdown by photosynthesis.

Precipitation is inferred to increase by 4,540 yr B.P., as the A:C increases to 0.6. While the geochemical signal remains largely unchanged, there is a nearly 1.0% increase

in TOC, which most likely reflects higher primary productivity, better preservation of organic matter, or a combination of both. It is possible that Convict Lake was transgressing at ~ 4,540 yr B.P., which led to colder, more anoxic bottom waters, improving the preservation potential which ultimately resulted in higher TOC, despite nearly unchanged $\delta^{15}N_{org,}$ $\delta^{13}C_{org}$ and C:N values from 4,770 to 4,540 yr B.P..

Before the transition into the late Holocene at 4,490 yr B.P., the A:C ratio shifts to -1.0, and the only important taxon aside from *Pinus* in the pollen spectra are *Abies*, Poaceae, Amaranthaceae, and *Quercus*. Taxa present in miniscule quantities include Ericaceae, which are only found in acidic, dry environments (Stevens et al., 2004). There is also a dramatic geochemical shift at this interval, with $\delta^{13}C_{org}$ increasing from -24.7 ‰ at 4,540 kyr B.P. to -14.5 ‰ at 4,490 kyr B.P., and C:N increasing from 10.7 to 18.5, respectively. $\delta^{15}N_{org}$ remains largely unchanged around 3.7 ‰. The higher C:N across this transition indicates that OM provenance for the lake was increasingly influenced by terrestrial sources. The $\delta^{13}C_{org}$ value appears to reflect the increased presence of C4 grasses in the watershed and supports the interpretation that the climate was warmer and drier in this interval. Convergence of these data suggest that Convict Lake most likely experienced a regression during at this time due to warmer, drier climate. With a warmer climate, it is plausible that the lake was frozen for a shorter interval, with a concomitant early onset of spring thaw and summer stratification. If this scenario were valid, lower nutrient availability to algae might help to explain decreases in TOC and TN values for this interval. These limnological conditions, paired with a transition to a more chaparral rich understory in the watershed are consistent with a warm, dry period. Similarly, low lake levels were observed at Mono Lake ~ 4,500 yr B.P., right before the transition to the

late Holocene (Zimmerman et al., in rev.). Mensing et al. (2004) observes a warm and dry Great Basin from 4,700 – 4,300 yr B.P. that was indicated by low A:C in the pollen record and higher values in the $\delta^{18}O$ record of Pyramid Lake. High magnetic susceptibility and enriched $\delta^{13}C_{org}$ measured on the sedimentary record of Fallen Leaf Lake (CA), which is situated adjacent to Lake Tahoe and ~250 km to the northwest of Convict Lake, also provides evidence for warm and dry conditions in the region 5,000 ~ 4,700 yr B.P. (Noble et al., 2016).

4.4 Late Holocene (4,490 kyr B.P. - present)

The late Holocene encompasses half of all pollen zones for the Convict Lake record and exhibits the most fluctuation both in the vegetation and geochemical signals. Immediately following the hot and dry period at the end of the mid-Holocene, our pollen-inferred vegetation reconstruction indicates a strong likelihood for a progressive transition to wetter and cooler climatic conditions with the A:C becoming positive at 3,890 yr B.P. Other important taxa are observed during this interval including *Abies, Quercus*, *Betula occidentalis*, *Artemisia* and Poaceae. This transition to a cooler, wetter climate in the beginning of the late Holocene is also observed in Zimmerman et al. (in rev), Mensing et al. (2004), and Noble et al. (2016). The geochemical signal for this period exhibits a trend of increasing TOC and TN, while $\delta^{13}C_{org}$ falls. The C:N values are around 11 at this time, consistent with an OM provenance where algae dominated. $\delta^{15}N_{org}$ is variable but remains in a range indicative of moderate-high paleoproductivity, which is an interpretation supported by the increase in TOC and TN. It is most likely that the seasonal melting of ice and summer stratification were delayed during this interval,

allowing for increased vertical nutrient flux, thus leading to higher primary production and possibly explaining the decline in $\delta^{13}C_{org}$ as depleted DIC is cycled into the photic zone. Similar processes of extended ice cover leading to increased DIC and DIN availability for primary production have been observed in Lake Nattmalsvatn in arctic Norway (Janbu et al., 2011), and in Fallen Leaf Lake, California (Noble et al., 2016). Vegetation and geochemical markers suggest that this neopluvial period lasted until at least ~3,510 yr B.P. at Convict Lake, which may have reached a water level highstand.

Zimmerman et al. (in rev) interpreted deepwater conditions at Mono Lake between 3,965 and 3,780 yr B.P., which coincides with Dechambeau Ranch highstand documented by Stine (1990), and the cool and wet conditions inferred at Convict Lake from 4,190 – 3,510 yr B.P.. This period represents the climate-shift that affected most of the northern hemisphere, when glaciers that had fully receded in the terminal Pleistocene began to reappear from Alaska to the southern Sierras, and the Intertropical Convergence Zone (ITCZ) moved southward as a result (Barclay et al., 2009, Davis et al., 2009, Bowerman and Clark, 2011, Zimmerman et al., in rev). This late Holocene high amplitude displacement of the ITCZ was recorded in the highly sensitive Cariaco Basin (offshore Venezuela) sediments, in which differences in seasonal sedimentation are directly controlled by ITCZ movements and atmospheric teleconnections to El Niño Southern Oscillation Events (Haug et al., 2001). There is strong evidence that the Little Ice Age (LIA) also induced a southward shift of the ITCZ (Haug et al., 2001), which is an interval known to have affected Sierra Nevada hydroclimate by causing another glacial advance (the so-called Matthes advance), and which is captured as a lithostratigraphic transition at 109 cm blf in Convict Lake (McGlue et al., in prep). Prior to the LIA, the

Mono Lake record indicates that mid Holocene aridity observed from 8,000-7,000 yr B.P. coincides with the most northerly position of the ITCZ (Zimmerman et al., in rev). Chiang and Bitz (2005) state that southerly displacement of the ITCZ can be interpreted as a balanced response of Hadley circulation in transporting atmospheric energy northwards to compensate for a loss of energy in the northern hemisphere high latitudes due to increased ice cover, whereas the opposite is true for northerly displacement of the ITCZ. In the case of a southerly displacement of the ITCZ, cooling over the extratropical North Atlantic results in simulated cooling over all of the Northern Hemisphere and southerly displacement of the tropical rainbelt (Lee et al., 2011; Chiang et al., 2014). This results in a weakened southern Hadley cell and a strengthened northern Hadley cell, and as a result, the southern wintertime subtropical jet weakens while the northern wintertime subtropical jet is strengthened (Chiang et al., 2014). As for the western United States, a strengthened northern wintertime subtropical jet directly results in more winter precipitation (Chiang et al, 2014). Thus, displacement changes in mean position of the ITCZ and increased ENSO activity may explain the increased frequency of high amplitude changes observed in the late Holocene pollen record at Convict Lake, relative to the Early and Middle Holocene.

Geochemical and pollen data indicate a cool and wet environment prevails and Convict Lake 3,510– 1,520 yr B.P.. Notable vegetation changes for this interval are the decrease in Poaceae, consistent presence of Asteraceae, Rhamnaceae, and the presence of *Tsuga mertensiana* from 2,750 to 1,580 yr B.P. *Tsuga mertensiana* reaches the critical point of >1% at 2,370 yr B.P., and at 1,700 kyr B.P., indicating that the cool, wet climate at Convict Lake led to the presence of a subalpine forest (Anderson and Davis, 1988).

Today, subalpine forests can only be found above the 2,393 m a.s.l. elevation of Convict Lake (Anderson and Davis, 1988). There is little evidence for cool, wet conditions in the Sierras during this time period. However, Bowerman and Clark (2011) interpreted a potential glacial advance at 2,800 yr B.P., and two additional advances of glacial ice at ~2,200 and ~1,600 yr B.P., in the North Fork of Big Pine Creek (central Sierra Nevada). Our results appear to confirm the hypothesis of Bowerman and Clark (2011) regarding the existence of glacial advances in the mid-late Holocene. The geochemical signal for this period is characterized by relatively high TOC, TN, and $\delta^{15}N_{org}$ values, and low C:N. We interpret the pollen and geochemical data to implicate a cold and productive Convict Lake for this period.

There are some fundamental differences between the climate conditions recorded in parts of the Great Basin and the eastern Sierras in the late Holocene. Mensing et al. (2013) state that the central and southern Great Basin were exceptionally dry, while the northernmost Great Basin was exceptionally wet from 2,800 to 1,850 yr B.P, inferring that this period of late Holocene aridity was confined to 40-42°N latitude, and that south of 40 °N experienced persistent dry climate and sites north of 42°N experience persistent wet climate. Convict Lake is located at 37 °N, and inferred paleoclimate for this interval is cool and wet, which is contradictory to these findings. The presence of *Tsuga mertensiana* at 2,370 yr B.P., and 1,700 kyr B.P. indicates that at Convict Lake, there is an absence of a hot and dry climate during this period, and conditions are more aligned with what is observed in the northernmost Great Basin (Mensing et al., 2013). Although the pollen records of Barret Lake (2,816 m.a.s.l, east side of Mono County), Starkweather Pond (2,438 m.a.s.l, west side, Madera County) and Tioga Pass Pond (3,018 m.a.s.l,

Sierran crest, Mono County) are not highly resolved in time, those vegetation records are dominated by subalpine and upper montane taxa, thus they also lack evidence of a hot and dry period at other high-altitude lakes within the Sierras during this interval (Anderson, 1990). The presence of *Tsuga mertensiana* in conjunction with the results of Anderson (1990) leads us to conclude that Convict Lake was cold and wet during this period.

Following the cold and wet period at Convict Lake that lasted until ~1,520 yr B.P., pollen and geochemical data transition and vary widely, which we interpret as evidence for a fluctuating hydroclimate that lasted until ~690 yr B.P.. At 1,520 yr B.P., *Pinus* content plummeted to 65% and other important taxa include *Artemisia*, Asteraceae, Amaranthaceae, Poaceae, *Erigonum*, and *Quercus*. These data indicate the possibility of a regression in Convict Lake. At this time, the A:C was negative (-0.42), supporting the interpretation of a transient warm and dry period. The geochemical signal is more complex at this time, and the stratigraphy shows the presence of mass wasting deposits affecting deepwater sedimentation (McGlue et al., in prep). TOC, TN and C:N are extremely low, which is likely the result of dilution from the influx of terrigenous grains. The $\delta^{13}C_{org}$ is enriched at -17‰ and the $\delta^{15}N_{org}$ reaches a record high of 6.0 ‰; these values are difficult to interpret and may reflect contributions from allochthonous and heavily altered Paleozoic OM. The same is true for the immediately overlying sediments (to ~1,350 yrs B.P.), which show slightly higher C:N (12.5-13.8) but similar $\delta^{13}C_{org}$ and $\delta^{15}N_{org,}$ and similarly negative A:C values. If the pollen-inferred climate signal is accurate for this time interval, it is plausible that lower lake levels and precipitation falling as rain instead of snow would drive sediment-laden plumes to enter Convict Lake and ultimately

transform into debris flows and turbidity currents. Further research on the interval is needed in order to draw further conclusions from the isotope data.

At 1,150 yr B.P., the paleoclimate is interpreted to be cool and wet, due to an A:C of 0.18. *Pinus* makes up an overwhelming 92% of taxa at this particular interval, and the only other taxa that could be considered significant are *Abies*, *Artemisi*a, and *Quercus*. There is a small amount of *Tsuga mertensiana*, 0.7%, indicating that subalpine forest was present at a higher elevation within the Convict Creek drainage basin, most likely within 500 m of the lake (Anderson and Davis, 1988). The pollen indicates that the regional paleoclimate must have been cooler with more winter precipitation than what is observed today, given the presence of *Tsuga mertensiana.* The geochemical signal is again decoupled from what the pollen record is suggesting. $\delta^{13}C_{org}$ becomes significantly enriched at -11.2 ‰, the $\delta^{15}N_{org}$ is 2.4 ‰ and the C:N ratio increases significantly to 39, indicating that mainly terrestrial biomass is contributing to the OM pool (Brodie et al., 2012). Increased winter precipitation most likely led to increased erosion of allochthonous OM to the lake during springtime runoff, including plant material and OM rich Paleozoic shale from the Mount Aggie and Convict Lake formations. Magnetic susceptibility and TIC values for this interval are high (McGlue et al., in prep), which further supports the interpretation of increased allochthonous material entering the basin as a root cause of the decoupling of pollen and geochemical values.

At 1,060 yr B.P., important taxa include *Abies*, *Betula*, Amaranthaceae, *Quercus*, and other TCT types. The A:C is -0.81, and there is a minute presence of *Ephedra*, which is only encountered in arid environments (Loera et al., 2012). Geochemically, $\delta^{15}N$ is 2.5‰, $\delta^{13}C_{org}$ is -27.9 ‰, and the C:N ratio is 9.5. The TOC value is 4.1 wt%. While the

pollen indicates a warm and dry paleoclimate, the geochemical signal suggests a productive lake with good conditions of OM preservation. We interpret these data to indicate the aridity suggested by the pollen was relatively modest, and probably did not result in a major water level change. Climate was more likely fluctuating with low amplitude changes through this interval of the late Holocene, as we interpret a cool and wet paleoclimate at 1,150 yr B.P. and at 1,010 B.P., which indicates climate variability at centennial scale.

At 1,010 yr B.P., the $\delta^{13}C_{org}$ is relatively enriched, while $\delta^{15}N_{org}$ and C:N increase, and TOC decreases. The pollen record at this interval exhibits some important changes relative to the underlying sample at 1,060 kyr B.P.. *Artemisia* abundance increased from 0.2 to 1.4%, and there is a minute presence of *Tsuga mertensiana* at 0.2%. This indicates that the elevation limit for the subalpine forest shifted downslope (Anderson and Davis, 1988). There is further evidence for increased precipitation in the TIC data for this interval in McGlue et al. (in prep). TIC is high, which most likely indicates an increased amount of winter precipitation and thus high amounts of springtime discharge from Convict Creek, leading to pulses in allochthonous material to the basin, resulting in the high TIC and low TOC due to dilution. This is further supported by the high C:N ratios which indicate terrigenous input to the lake (Meyers and Terranes, 2001).

At 970 yr B.P., we interpret that the paleoclimate at Convict Lake was cold and wet. *Artemisia* percentages nearly double from their level at 1,060 yr B.P., resulting in a positive A:C, and *Tsuga mertensiana* reaches 1.4%, indicating that a subalpine forest had fully encroached the area surrounding Convict Lake. $\delta^{13}C_{org}$ becomes strongly depleted, while the C:N ratio for this interval is 9.8, and $\delta^{15}N$ decreases to 2.5 ‰, indicating that

organic matter provenance for the lake transitioned back to being algal dominant and efficient vertical nutrient cycling was occurring in deep water (Meyers and Terranes, 2001). This cool and wet phase lasted until ~690 yr B.P.. Notably, *Tsuga mertensiana* is present at 0.2% at 800 yr B.P. and 690 yr B.P, further supporting the interpretation of a cold and wet paleoclimate.

At 650 yr B.P., the A:C is -0.3, and at 600 yr B.P. the A:C can be considered 0, for neither Amaranthaceae or *Artemisia* were present to be counted. There is very little diversity in vegetation during this interval, but there is 0.4% *Tsuga mertensiana* at 600 yr B.P. This presence of *Tsuga mertensiana* coincides with the timing of the inception of the LIA in the eastern Sierras (Curry, 1971, Wood, 1977, Stine, 1994, Gillespie and Clark, 2011). $\delta^{13}C_{org}$ is incredibly enriched ~ 650 – 600 yr B.P., which mirrors the $\delta^{13}C_{org}$ value response recorded in Fallen Leaf Lake for the LIA (Noble et al., 2016).

For the remainder of late Holocene, A:C ratios are positive, and *Artemisia* percentages reach record highs. We interpret the data to indicate that the last ~ 550 years have exhibited the cold, wet winters and warm, dry summers that currently prevail in the region, due to the similarity of the pollen record to what is presently observed growing on the landscape and within the Convict Creek drainage basin. The geochemical data supports this interpretation, pointing to a productive lake that resulted from nutrient fluxes occurring in the spring months when the ice has melted and the lake has mixed. f

However, since the industrial revolution (last ~ 150 yrs), $\delta^{15}N_{org}$ has significantly decreased to below 1.0 ‰, whereas $\delta^{13}C_{org}$, C:N, and TOC values have increased, which we interpret as the impacts of warming and increased anthropogenic activity in the Convict Lake watershed (Mann et al., 1999; Crowley, 2000). This warming has most

likely led to shorter intervals of water column mixing, leading to prolonged periods of deep stratification, in which nutrients were sequestered in the hypolimnion and recirculation into the epilimnion was limited (Smol et al., 2005). This, paired with warmer water temperatures in the summer months, lead us to interpret that algal composition may be changing at Convict Lake, potentially favoring N_2-fixing blue-green algae, and thus explaining the low $\delta^{15}N_{org}$ values and high TOC values. It is possible that this transition was influenced by two other factors: 1) increased phosphorus and nitrogen input to the lake via human activity immediately surrounding the basin, and 2) increased atmospheric input of N_2. The latter phenomenon has been observed in many North temperate subarctic lakes (O' Neill et al., 2012, Taranu et al., 2012, Taranu et al., 2015). Taranu et al. (2015) analyzed cyanobacterial activity over the last 200 years in 108 lakes, 27 of which were temperate to subarctic, and found that 58% of lakes had significant increases in cyanobacterial pigment concentrations, with a large portion of observed increases happening post 1940 C.E.. Regression tree analysis of the data compiled by Taranu et al. (2015) revealed that both increases in nutrient concentration and warmer air temperatures were significant predictors of the magnitude of change in blue-green algae productivity. As the climate continues to warm, it is likely that not only Convict Lake but other alpine lakes within the Sierras could witness fundamental changes in their ecology due to harmful blue-green algae blooms (Taranu et al., 2015) which will lead to the damage of fish communities that attract millions of visitors each year.

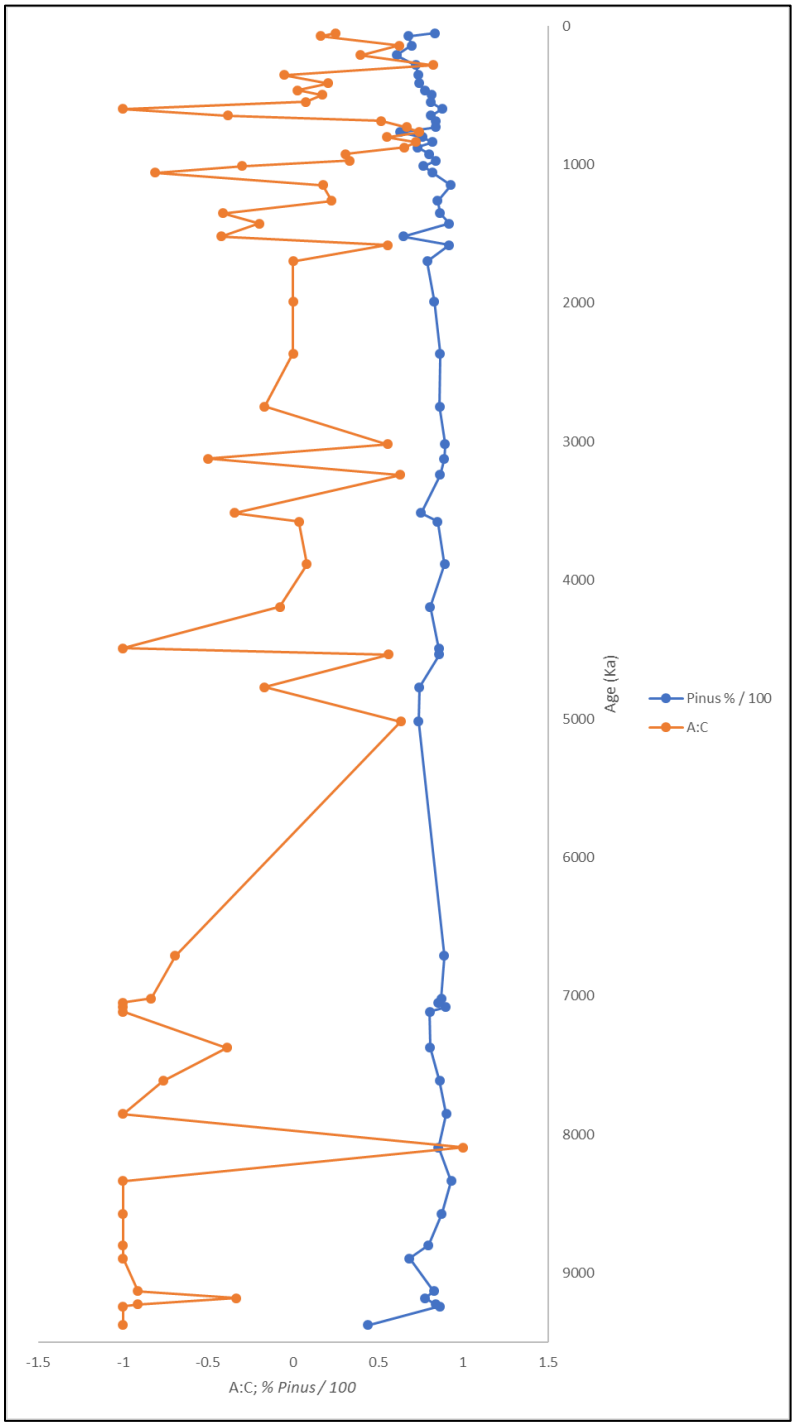

Figure 11. Generally, increases in pine pollen coincide with increases in the A:C while decreases in pine pollen coincide with a more negative A:C. Total *Pinus* values were divided by 100 for visualization purposes.

5. Conclusions

This study provides valuable insight into the paleoclimate and vegetation history of the eastern Sierra Nevada and the Convict Creek drainage basin.

- In the early Holocene (9,380 – 8,890 yr B.P.) the pollen record captures the initial vegetation response to glacial retreat and the genesis of Convict Lake. A montane chaparral forest was established, with abundant Amaranthaceae and Poaceae. This initial response is most likely reflective of poor soil quality due to the recent glacial recession and a relatively warm and dry climate. This interpretation is made because chaparral taxa dominate from the early Holocene until the middle Holocene. Geochemical data support this interpretation, with low average TOC values, and high $\delta^{13}C_{org}$ and C:N values. Together the data suggest that lake level was most likely lower than the present day.
- As observed in other pollen and proxies records, the Middle Holocene appears to be a period of vegetation stability in the Convict Lake record, in evidence from largely invariant pollen and geochemical data that lack major high amplitude excursions. The climate is interpreted to have become considerably wetter and cooler during this period, which is inferred by the presence of *Tsuga mertensiana*, which indicates the encroachment of the subalpine forest to lower altitudes in the Convict Creek drainage basin. The first shift of A:C to a positive value is also observed during this period. By the end of the Middle Holocene and

moving into the Late Holocene, climate does briefly become warmer and drier, marked by the presence of the indicator species Ericaceae, as well as a shift in A:C from 0.5 to -1.

- Convict Lake experienced high amplitude variability in hydroclimate during the Late Holocene. The southward shift of the ITCZ that induced the Dechambeau Ranch highstand at Mono Lake ~ 3,965 – 3,780 yr B.P. appears to have also affected temperature and precipitation at higher elevations, for a distinct shift in the Convict Lake pollen and geochemical record that indicates wetter and cooler conditions is recorded from ~ 4,190 – 3,510 yr B.P.. Thus, high amplitude variability in the Late Holocene can probably be explained by high frequency shifts in the ITCZ driven by North Atlantic sea surface temperatures and sea ice extent, as well as increased ENSO activity. Presence of the important indicator species, *Tsuga mertensiana*, coincides with potential late Holocene (~ 2,800, 2,200, 1,600 yr B.P.) glacial advances recorded by Bowerman and Clark (2011) in the central Sierra Nevada.
- There is considerable climatic variability ~ 1.6 – 0.6 kyr B.P., as inferred from the vegetation reconstruction. The geochemical signal is often decoupled from the pollen record, due to mass wasting and transport of OM-rich sediments to the lake's depocenter. Further investigation of the stratigraphy of cores recovered from the lake are required to fully understand these dynamics.

- Since the industrial revolution, it is likely that blue-green algae have begun to thrive in Convict Lake, as observed in other alpine lakes. It is likely that this activity is being driven by increased N_2 input to the lake from atmospheric warming, and prolonged periods of deep-water column stratification. This presents a threat to the fish communities that drive a large sector of the tourism industry in the eastern Sierras.

APPENDIX A

Pollen Counts (%)

Depth	Age	Abies	Alnus	Artemisia	Asteraceae	Betula	Chenopodium
0	53	5.2	0.2	1	0.2	2.1	0.4
2.5	72	3.2	0.5	2.5	0.2	4.8	1.6
12.5	143	3.2	0	4.3	0	1.9	0.5
22.5	211	1.2	0	3.7	0.9	3.2	1.4
32.5	283	1.6	0	6.2	0.7	5.5	0.2
42.5	355	1.5	1.3	3.6	0.3	4.6	2
52.5	414	3.7	0.7	3.5	0	4.9	2.1
62.5	463	2.6	0	1.9	0.5	3.5	1.6
72.5	498	2.2	0.2	2.4	0.2	2.9	1.5
82.5	548	3.1	0.2	1.4	0.4	4.1	1
93	600	6.5	0.2	0	0	0.7	0
103	647	4.2	0.2	1.2	3.7	0.7	2.2
113	685	3.1	0.2	2.2	0.7	2.9	0.5
125.5	730	3.9	0	2.5	0.5	2.3	0.5
135.5	765	2.6	0	8.1	0.7	6.9	1
145.5	801	1.7	0	6.6	0.2	3.5	1.2
155.5	837	3	0	5	0	2.5	0.8
165.5	876	1	0.2	6.7	0	3.5	1.2
175.5	924	0.7	0.2	1.9	0.7	4.1	1
185.5	972	1.4	0.2	2.8	0.2	2.1	0.7
195.5	1010	1.4	0.2	1.4	0.7	4.1	1.2
205.5	1058	2.1	0	0.2	0.2	5.2	1.9
217.5	1148	1.7	0	1	0.5	0.2	0.7
227.5	1261	1.9	0.2	1.9	0.2	1.7	0.2
237.5	1351	2.2	0	0.5	0	1.5	1.2
244.5	1427	0	0.4	0.4	0	1.6	0.6
259.5	1520	1.7	0.5	1.5	1	11.3	3.7
269.5	1583	2.5	0	0.7	0.2	0.5	0.2
279.5	1698	1.2	0.2	1.4	0.2	2.4	1.4
289.5	1990	0.8	0.2	1	0.4	2.7	0.8
299.5	2365	1.7	0	0.6	0.6	1.9	0.2
309.5	2747	3.7	0	0.5	0.2	0.9	0.7
319.5	3017	1.7	0	0.7	0.2	1.7	0.2
329.5	3124	0.9	0	0.7	0.5	1.6	2.1
339.5	3239	1.2	0	2.2	0.2	1.2	0.5
349.5	3514	1.5	0	1.9	0.2	6.5	2.9

351.5	3577	1	0	1.5	0.2	2.7	1.2
361.5	3886	0.5	0.2	2	0	2	1.7
371.5	4191	1.2	0.2	1.2	0.2	2.1	0.7
381.5	4492	1.4	0	0	0	5.1	1.2
391.5	4536	0.5	0	2.5	0.2	0	0.2
401.5	4772	0.2	0.2	1	0.5	2.5	0.7
411.5	5021	0.3	0	4.9	1.6	4.4	1.1
480	6710	1.6	0	0.2	0.2	1.1	0.9
490	7017	1.7	0.2	0.2	0.2	2.7	1.7
500	7049	3	0	0	0	0.9	1.2
510	7081	0.5	0	0	0	0.5	0.5
520	7113	1.2	0	0	0	0	1
530	7373	0.2	0.2	1.5	0.5	1.7	3.2
540	7612	0.5	0	0.2	0.2	1.2	1.5
550	7852	0.8	0	0	0	1.3	1.7
560	8094	0.5	0	0.5	0.7	3.7	0
570	8336	1.3	0	0	0	0	1.7
580	8571	0.9	0	0	0	0.2	2
589.5	8799	0.2	0	0	0	0	3.6
600	8894	0.2	0	0	1	0	3.9
610	9130	0	0	0.2	0.7	0.2	4.4
620	9182	0	0	1.6	3.2	3.2	3.2
630	9226	0.5	0	0.2	0.2	0	4.3
635	9242	0	0	0	0	0	6.3
645	9375	0	0	0	0.4	0	4.5

Depth	Age	Corylus	Ephedra	Ericaceae	Eriogonum	Juglandaceae
0	53	0	0	0	0	0
2.5	72	0	0	0	0	0
12.5	143	0	0	0.5	0	0
22.5	211	0	0	0.2	0	0
32.5	283	0	0	0.2	0	0
42.5	355	0.3	0.5	0.3	0	0
52.5	414	0	0	0	0	0
62.5	463	0	0.5	0.5	0	0
72.5	498	0	0.2	0	0	0
82.5	548	0	0.4	0	0	0
93	600	0	0	0	0	0
103	647	0	0.2	0	0	0
113	685	0	0	0	0	0

125.5	730	0	0	0	0.5	0
135.5	765	0	0.7	0	0.5	0
145.5	801	0	0	0	0.5	0
155.5	837	0.3	0	0	0.5	0
165.5	876	0	0.5	0	0.5	0.2
175.5	924	0	0.2	0	1.2	0.2
185.5	972	0	0	0	0	0.2
195.5	1010	0.2	0.2	0	0.5	0.2
205.5	1058	0	0.5	0	0	0
217.5	1148	0	0	0	0.2	0
227.5	1261	0	0.2	0	0.2	0
237.5	1351	0	0	0	0	0.7
244.5	1427	0	0.4	0.2	0	0.4
259.5	1520	0	0.7	0	1	0.2
269.5	1583	0	0	0	0.2	0
279.5	1698	0.2	0.7	0	1	0.2
289.5	1990	0	0	0	0	0.2
299.5	2365	0	0	0	0.2	0
309.5	2747	0	0	0	0	0.2
319.5	3017	0	0	0	0	0
329.5	3124	0	0	0	0	0
339.5	3239	0.2	0	0	0.2	0.2
349.5	3514	0	0	0	0.5	1
351.5	3577	0	0	0	0	0
361.5	3886	0	0	0	0	0
371.5	4191	0.5	0	0	0	0
381.5	4492	0	0	0.2	0.2	0
391.5	4536	0	0.7	0	0.2	0
401.5	4772	0.5	0	0	0	0.7
411.5	5021	0	0	0	0	0.3
480	6710	0	0.2	0	0.7	0
490	7017	0	0	0	0	0
500	7049	0	0.5	0	0	0
510	7081	0	0.5	0	0.2	0
520	7113	0	0.2	0	0.5	0
530	7373	0	0.2	0	0.5	0
540	7612	0	0.2	0	0	0
550	7852	0	0.2	0	0.2	0
560	8094	0	0.2	0	0.5	0
570	8336	0	0	0	0	0
580	8571	0	0.2	0	0	0.2
589.5	8799	0	0.2	0	0	0.2
600	8894	0	0.2	0	0	0.2

610	9130	0	0.2	0	0	0
620	9182	0	0	0	0	0
630	9226	0	0	0	0	1
635	9242	0	0	0	0	0
645	9375	0	0	0	0.4	0

Depth	Age	Malvaceae	Onagraceae	Ophioglossaceae	Pinus	Poaceae
0	53	0.2	0	0	83.6	1.3
2.5	72	0	0	0	67.9	2.9
12.5	143	0	0	0	69.7	4.8
22.5	211	0	0	0	60.9	1.6
32.5	283	0	0	0	72.1	0.9
42.5	355	0	0.3	0	73.8	0.8
52.5	414	0	0	0	74	2.3
62.5	463	0	0	0	77.6	2.4
72.5	498	0	0	0	81.4	2.2
82.5	548	0	0	0	80.8	0.8
93	600	0	0	0	87.7	1.3
103	647	0	0	0	81	2.7
113	685	0	0.2	0	83.9	2.2
125.5	730	0	0	0	83.9	1.1
135.5	765	0	0	0	63.1	3.8
145.5	801	0	0	0	75.9	1.7
155.5	837	0	0	0	82	1.3
165.5	876	0	0	0	73.1	1.7
175.5	924	0	0	0	80.1	3.6
185.5	972	0	0	0	84	0.9
195.5	1010	0	0	0	76.7	0.7
205.5	1058	0	0	0	82.1	0.7
217.5	1148	0	0	0	92.7	0.5
227.5	1261	0	0	0	85	1
237.5	1351	0	0	0	86.5	0.2
244.5	1427	0	0	0	91.9	0.2
259.5	1520	0	0	0	64.9	1
269.5	1583	0	0	0	91.9	0
279.5	1698	0	0	0	78.9	1.2
289.5	1990	0	0	0	83.1	1
299.5	2365	0	0	0	86.5	0.4
309.5	2747	0	0	0	86.2	0.9
319.5	3017	0	0	0	89.4	1.4

329.5	3124	0	0	0	88.8	0.9
339.5	3239	0	0	0	86.5	1.7
349.5	3514	0	0	0	75.3	1.2
351.5	3577	0	0	0.5	85	1.5
361.5	3886	0	0	0	89.2	1.2
371.5	4191	0	0	0	80.7	4.4
381.5	4492	0	0	0	85.8	2.2
391.5	4536	0	0	0	86	2.9
401.5	4772	0	0	0	74.3	14
411.5	5021	0	0	0	73.8	1.6
480	6710	0	0	0	88.9	0.9
490	7017	0	0	0	87.3	1
500	7049	0	0	0	85.2	5.2
510	7081	0	0	0.2	89.6	5.1
520	7113	0	0	0	80.4	15.3
530	7373	0	0	0	80.5	3.7
540	7612	0	0	0	86.1	3.9
550	7852	0	0	0.4	90	0.8
560	8094	0	0	0.2	85.4	1.7
570	8336	0	0	0	93.1	1.7
580	8571	0	0	0.7	87.4	3.3
589.5	8799	0	0	0.2	79.6	8.6
600	8894	0	0	0.2	68.5	17.3
610	9130	0	0	0.2	82.8	1
620	9182	0	0	0	77.8	3.2
630	9226	0	0	0	83.7	1.2
635	9242	0	0	0	86.2	1.9
645	9375	0	0	0	44.2	44.6

Depth	Age	Polypodiaceae	Populus	Quercus	Rhamnaceae	Rosaceae
0	53	0	0	3.6	0.4	0
2.5	72	0	0	9.5	0	0
12.5	143	0	0	11	0	0
22.5	211	0	0	20.4	0	1.2
32.5	283	0	0	9.1	0.7	0
42.5	355	0	0	6.9	0.5	0
52.5	414	0	0	5.8	0.9	0
62.5	463	0	0	6.8	0.2	0
72.5	498	0	0	3.3	1.8	0
82.5	548	0	0	5.4	0.8	0
93	600	0	0	2	0.4	0

103	647	0	0	2.2	1	0
113	685	0	0	2.4	0.5	0
125.5	730	0	0	4.1	0.5	0
135.5	765	0	0.7	7.6	1.2	0
145.5	801	0	0	4.7	2.4	0
155.5	837	0	0	2.5	1	0
165.5	876	0	0	9	0	0
175.5	924	0	0	4.9	0	0.2
185.5	972	0	0.2	4.2	0.5	0.2
195.5	1010	0.5	0.2	4.6	1.9	0
205.5	1058	0	0	4.2	0.9	0
217.5	1148	0.2	0	1.2	0.2	0
227.5	1261	0.2	0	4.8	0.5	0
237.5	1351	0	0	5.7	0	0
244.5	1427	0	0	2	0.4	0
259.5	1520	0.2	0.2	11.3	0	0
269.5	1583	0	0	3.4	0	0
279.5	1698	0.5	0	5.7	1.4	0
289.5	1990	0.2	0	7.2	0.2	0
299.5	2365	0	0	4.5	0.2	0
309.5	2747	0	0	5.4	0.5	0
319.5	3017	0	0	3.8	0.5	0
329.5	3124	0	0.2	3	0.2	0
339.5	3239	0	0.2	4.4	0.5	0
349.5	3514	0	0	5.3	0.2	0
351.5	3577	0	0	4.7	0	0.2
361.5	3886	0	0	2.5	0	0
371.5	4191	0.5	0	3.7	0	0
381.5	4492	0	0	0	0	0
391.5	4536	0.5	0	4.2	0	0
401.5	4772	0.5	0	2.5	0	0
411.5	5021	0	0	6.8	0.8	0
480	6710	0	0	4.4	0	0
490	7017	0	0	3.4	0.2	0
500	7049	0	0	2.3	0	0
510	7081	0	0	1.9	0	0
520	7113	0	0	1	0	0
530	7373	0	0	6.9	0.2	0
540	7612	0	0	5.9	0	0
550	7852	0	0	3.5	0.2	0
560	8094	0	0	5.4	0.2	0
570	8336	0	0	1.1	0	0
580	8571	0.2	0	4	0.2	0

589.5	8799	0	0	5	0.2	0
600	8894	0	0.2	6.8	0	0
610	9130	0.7	0	9.1	0	0
620	9182	0	0	0	0	0
630	9226	1.4	0	3.6	0.2	0
635	9242	0.2	0	3.5	0.2	0
645	9375	0.7	0	4.9	0	0

Depth	Age	Rumex	Sarcobataceae	Sequoia	Taxaceae	Tsuga
0	53	0	0.2	0	0.8	0
2.5	72	0	0.2	0	0	0
12.5	143	0	0.5	0	0.5	0
22.5	211	0	0.2	0.7	0.5	0
32.5	283	0	0.4	0	1.6	0
42.5	355	0	2	0	1	0.3
52.5	414	0	0.2	0.7	0.5	0
62.5	463	0	0.2	0	1.4	0
72.5	498	0	0.2	0	0.7	0
82.5	548	0	0.2	0	0.4	0.2
93	600	0	0.2	0	0.2	0.4
103	647	0	0.5	0	0	0
113	685	0	0.2	0	0.5	0.2
125.5	730	0	0	0	0.2	0
135.5	765	0	0.2	0	0.7	0
145.5	801	0	0.7	0	0.5	0.2
155.5	837	0	0	0	1.3	0
165.5	876	0	0.2	0	1.2	0
175.5	924	0	0	0	0	0
185.5	972	0	0.7	0	0	1.4
195.5	1010	0	1.4	0	0	0.2
205.5	1058	0	0	0	1.2	0
217.5	1148	0	0	0	0.2	0.5
227.5	1261	0	1	0	0	0
237.5	1351	0	0	0	0.7	0
244.5	1427	0	0	0	0.4	0.6
259.5	1520	0	0	0	0	0
269.5	1583	0	0	0	0	0.2
279.5	1698	0	0	0	0.7	1.9
289.5	1990	0	0.2	0	0.2	0.8
299.5	2365	0	0.4	0	0.6	1.5
309.5	2747	0	0	0	0	0.5
319.5	3017	0	0	0	0.2	0

329.5	3124	0	0	0	0	0
339.5	3239	0	0	0.2	0	0
349.5	3514	0	1	0	0.5	0
351.5	3577	0	0.2	0	0	0.5
361.5	3886	0	0	0	0	0
371.5	4191	0	0.7	0	0.7	0
381.5	4492	0	0.5	0	0.2	0
391.5	4536	0.2	0.5	0	0	0
401.5	4772	0	0.7	0	0.2	0
411.5	5021	0	0	0	0.8	0.3
480	6710	0	0.2	0	0	0.2
490	7017	0	0.5	0	0	0
500	7049	0	0.2	0	0.2	0
510	7081	0	0.5	0	0	0.2
520	7113	0	0.2	0	0	0
530	7373	0	0.2	0	0.2	0
540	7612	0	0	0	0.2	0
550	7852	0	0	0	0.4	0
560	8094	0	0	0	0.2	0
570	8336	0	0	0	0.2	0
580	8571	0	0	0	0	0
589.5	8799	0	0	0	0.2	0
600	8894	0	0.7	0	0	0
610	9130	0	0	0	0	0
620	9182	0	0	0	0	0
630	9226	0	0.2	0	1	0
635	9242	0	0	0	0	0
645	9375	0	0	0.4	0	0

Depth	Age	Unknown	A/C Ratio
0	53	0.6	0.25
2.5	72	6.8	0.162791
12.5	143	2.9	0.622642
22.5	211	3.9	0.396226
32.5	283	0.9	0.823529
42.5	355	0.3	-0.05263
52.5	414	0.7	0.206897
62.5	463	0.2	0.027027

72.5	498	0.7	0.170732
82.5	548	0.6	0.076923
93	600	0.2	-1
103	647	0	-0.38462
113	685	0.2	0.517241
125.5	730	0	0.666667
135.5	765	2.1	0.741935
145.5	801	0.2	0.552941
155.5	837	0	0.724138
165.5	876	0.7	0.654321
175.5	924	0.7	0.310345
185.5	972	0	0.333333
195.5	1010	3.4	-0.3
205.5	1058	0.7	-0.80952
217.5	1148	0	0.176471
227.5	1261	0.7	0.225806
237.5	1351	0.5	-0.41176
244.5	1427	0.4	-0.2
259.5	1520	0.7	-0.42308
269.5	1583	0	0.555556
279.5	1698	0.5	0
289.5	1990	0.8	0
299.5	2365	0.4	-9.3E-17
309.5	2747	0.2	-0.16667
319.5	3017	0	0.555556
329.5	3124	0.9	-0.5
339.5	3239	0.2	0.62963
349.5	3514	1.9	-0.34483
351.5	3577	0.7	0.034483
361.5	3886	0.7	0.081081
371.5	4191	3.3	-0.07692
381.5	4492	3.1	-1
391.5	4536	1.2	0.5625
401.5	4772	1.5	-0.16667
411.5	5021	3.3	0.633333
480	6710	0.4	-0.69231
490	7017	0.7	-0.83333
500	7049	1.2	-1
510	7081	0.2	-1
520	7113	0	-1
530	7373	0	-0.38776
540	7612	0	-0.76471
550	7852	0.4	-1

560	8094	0.5	1
570	8336	0.9	-1
580	8571	0.7	-1
589.5	8799	1.7	-1
600	8894	0.5	-1
610	9130	0.2	-0.91304
620	9182	7.9	-0.33333
630	9226	2.4	-0.91489
635	9242	1.6	-1
645	9375	0	-1

APPENDIX B

Bulk and Stable Isotope Geochemical Data

Composite depth (cm)	Sample wt (mg)	δ15NAIR (‰)	δ13CVPDB (‰)	Wt% N	Wt% C
2.5	25.374	0.7	-24.8	0.3	4.2
7.5	25.231	0.6	-23.8	0.4	4.5
12.5	20.1	0.9	-23.1	0.3	4.3
17.5	25.156	0.8	-19.1	0.2	4.2
22.5	21.024	1.2	-23	0.3	4.5
27.5	25.46	1.2	-28.4	0.4	4.2
32.5	25.007	1.9	-26	0.3	2.8
37.5	21.771	1.6	-27.8	0.4	3.4
42.5	18.305	1.5	-27.8	0.4	3.6
47.5	25.464	1.3	-29.2	0.4	4.2
52.5	23.818	1.6	-28.6	0.4	3.6
57.5	25.043	2.5	-24.1	0.3	3.2
62.5	25.465	1.4	-25.4	0.3	3.9
67.5	25.1	1.6	-28.1	0.4	3.2
72.5	16.116	1.6	-28.4	0.5	4.3
77.5	25.186	2.3	-27.5	0.3	2.6
82.5	15.95	2	-28.3	0.4	3.3
88	20.554	2.4	-28.5	0.3	2.8
93	25.706	2.7	-28.5	0.2	2.1
98	25.529	2.8	-9.6	0.1	3.3
103	21.042	1.7	-29.2	0.4	3.9
108	25.419	1.8	-27.8	0.4	3.4
110	25.423	1.7	-25.7	0.3	3.9
116.5	25.467	2	-26.5	0.3	3.6
122	25.275	0.8	-27.9	0.4	4.2
125.5	25.213	1.7	-25.7	0.4	4
130.5	25.278	2	-27.1	0.5	4.6
135.5	25.439	2.4	-27.7	0.4	3.4
140.5	25.115	2.5	-27.4	0.3	3.1
145.5	25.116	1.4	-28.8	0.5	4.4
150.5	25.404	1.9	-28.2	0.4	3.7
155.5	25.14	2	-28.3	0.4	3.7
160.5	24.979	2.1	-28.2	0.5	4.3
165.5	25.014	3.2	-24.3	0.2	2.3

170.5	25.768	1.9	-27.4	0.4	3.9
175.5	25.297	1.8	-28	0.5	4.6
180.5	25.346	2.4	-27.9	0.4	3.4
185.5	25.386	2.5	-28	0.3	3
190.5	25.094	3.9	-27.9	0.1	1.1
195.5	25.784	3.8	-15.9	0.1	3
200.5	25.549	2.5	-28.6	0.4	4.1
205.5	25.481	2.5	-27.9	0.4	4.1
210.5	25.14	3.1	-27.2	0.3	2.5
217.5	25.292	2.4	-11.2	0.1	3.9
222.5	25.402	2.5	-24.9	0.3	3.2
227.5	25.086	1.7	-27.7	0.4	3.7
232.5	25.227	2.5	-26.8	0.2	2.5
237.5	25.364	2.1	-22	0.3	3.8
242.5	25.282	2.6	-27.1	0.3	2.7
244.5	24.085	3.7	-21.3	0.2	2.2
249.5	25.122	3.8	-20.2	0.1	1.7
254.5	25.015	3.7	-26.8	0.2	1.7
259.5	25.67	6	-17.4	0	0.3
264.5	25.104	3.7	-25.5	0.2	2.5
269.5	25.059	3.9	-26.8	0.3	2.9
274.5	26.018	4.5	-9.9	0.1	3.5
279.5	24.861	2.6	-27.9	0.5	4.7
284.5	24.968	2.9	-26.9	0.4	3.7
289.5	24.286	2.5	-28.1	0.5	4.5
294.5	23.987	3.1	-27.3	0.4	3.6
299.5	25.087	3.3	-27.6	0.5	4
304.5	24.413	2.8	-26.8	0.4	3.7
309.5	25.335	1.8	-24.2	0.3	3.4
314.5	25.009	2.8	-27.3	0.4	4
319.5	25.013	3.1	-26.8	0.4	3.2
324.5	25.068	3.2	-27.4	0.4	3.6
329.5	25.106	2.7	-27.2	0.4	4.1
334.5	25.903	2.6	-23.3	0.4	4.1
339.5	24.781	3.2	-26	0.3	2.9
344.5	25.109	3.1	-27.3	0.4	3.9
349.5	24.549	2.8	-26.5	0.3	3
351.5	25.124	3.3	-26.8	0.3	3
356.5	25.202	3.3	-26.9	0.3	3
361.5	25.32	4.1	-22.9	0.1	1.7
366.5	25.051	3.4	-26.6	0.3	2.6

371.5	25.276	3.2	-27.4	0.2	2.3
376.5	25.715	4.3	-26.3	0.2	1.6
381.5	25.231	3.7	-14.5	0	0.7
386.5	25.372	4	-26	0	0.4
391.5	25.491	3.9	-24.7	0.2	2
396.5	25.07	4.1	-26.8	0.2	1.7
401.5	25.305	3.9	-26.3	0.1	1.3
406.5	25.101	3.9	-24.1	0.1	1.4
411.5	25.768	6.6	-23	0	0.4
416	25.119	4.1	-25.7	0.1	0.8
422.5	25.209	2.7	-25.1	0.1	0.9
427.5	25.513	2.5	-25	0.2	2.1
432.5	25.392	2.7	-24	0.2	2.3
437.5	25.339	3.2	-6.9	0	2.9
442.5	25.199	2.8	-24.7	0.1	1.3
447.5	25.807	3.4	-22.7	0.2	1.9
452.5	25.613	3.9	-25	0.1	1.6
480.5	25.084	2.9	-24.8	0.2	2.6
485.5	25.589	3.4	-26.7	0.3	3.2
490.5	25.308	4.2	-25.1	0.1	1.2
495.5	25.115	4.2	-24.3	0	0.5
500.5	25.269	3	-26.1	0.1	1.6
505.5	25.231	3.9	-25.8	0.2	2.1
510.5	25.336	4.8	-9.6	0.1	2.8
515.5	25.132	3.6	-25.6	0.1	1.1
520.5	25.464	4	-26.5	0.3	2.5
525.5	25.381	3.9	-26	0.1	1.5
530.5	25.114	3.1	-24.2	0.1	1.3
535.5	25.202	3.9	-26.1	0.1	1.6
540.5	25.45	3.2	-26.5	0.2	2
545.5	25.269	2.7	-25.5	0.1	1.6
550.5	25.317	4.2	-24.5	0.2	1.5
555.5	25.649	3.7	-26	0.2	1.7
560.5	25.253	4.2	-25.9	0.2	1.9
565.5	25.291	3.7	-26	0.1	1.4
570.5	25.342	3.9	-23.1	0.1	1.6
575.5	25.236	3.5	-26.1	0.1	1.5
580.5	25.204	4.3	-26.2	0.2	2.1
585.5	25.115	3.7	-23.4	0.1	1.5
589.5	25.475	4.1	-20.7	0.1	1.3
590.5	25.457	1.2	-9.8	0	2.2

595.5	25.469	3.6	-26.1	0.2	1.7
600.5	25.5	3.7	-21.6	0.1	1.4
605.5	25.177	2.9	-24.9	0.1	1.3
610.5	25.101	2.5	-21	0.1	1.1
625.5	25.246	3.1	-20.1	0	0.7
635.5	25.302	0.3	-24.1	0.1	1.3
640.5	25.1	2.2	-24	0.1	1.1
645.5	25.091	3.4	-17.9	0	0.8

References

Adam, D.P., 1967, Late-Pleistocene and Recent palynology in the central Sierra Nevada, California: Quaternary Paleoecology (Ed by E.J. Cushing & H.E. Wright, Jr). Yale University Press, New Haven, CT.

Adam, D.P., 1988, Palynology of two Upper Quaternary cores from Clear Lake, Lake County, California: U.S. Geological Survey Professional Paper, No. 1363. United States Geological Survey, Washington, D.C.

Adam, D.P., and West, G.J., 1983, Temperature and precipitation estimates through the last glacial cycle from Clear Lake, California, pollen data. Science, v. 219, p. 168-170.

Ali, G.A.H., 2018, Late Glacial and deglacial fluctuations of Mono Lake, California [Ph.D. thesis]: Columbia University, 255 p.

Anderson, R.S., Davis, O.K., & Fall, P., 1985, Late-glacial and Holocene vegetation change in the Sierra Nevada of California with particular reference to the Balsam Meadow site: Late Quaternary Vegetation and Climates of the American Southwest (Ed by B.F. Jacobs, P.L Fall & O.K. Davis), American Association of Stratigraphic Palynologists, Dallas, TX, p. 127-140.

Anderson, R.S., and Davis, O.K., 1988, Contemporary pollen rain across the Central Sierra Nevada, California, USA: Relationship to modern vegetation types: Arctic and Alpine Research, v.20, p, 448-460

Anderson, R.S., 1990, Holocene forest development and paleoclimates within the central Sierra Nevada, California: Journal of Ecology, v. 78, no.2, p. 470-489.

Bailey, R.A., Dalrymple, B.G., Lanphere, M.A., 1976, Volcanism, structure, and geochronology of Long Valley Caldera, Mono County, California: Journal of Geophysical Research, v. 81, n. 5, p. 725-744.

Bales, R.C., Molotch, N.P., Painter, T.H., Dettinger, M.D., Rice, R., and Dozier, J., 2006, Mountain hydrology of the western United States: Water Resources Research, v. 42, no. 8

Bales, R. C., Goulden, M. L., Hunsaker, C. T., Hartsough, P. C., O'Geen, A. T., Hopmans, J., and Safeeq, M., 2018, Mechanisms controlling the impact of multi-year drought on mountain hydrology: Scientific e Reports, v. 8, 690 p. https://doi.org/10.1038/s41598-017-19007-0.

Barclay, D. J., Wiles, G. C., Calkin, P. E., 2009, Holocene glacier fluctuations in Alaska: Quaternary Science Reviews, v. 28, no. 21-22, p. 2034-2048.

Berger, A., Loutre, M.-F., 1991, Insolation values for the climate of the last 10 million years: Quaternary Science Reviews, v.10, p. 297-317.

Betchelder, G.I., 1980, A late Wisconsinian and early Holocene lacustrine stratigraphy and pollen record from the west slope of the Sierra Nevada, California: American Quaternary Association, Abstracts with Program, v. 6, 13.

Blackwelder, E., 1931, Pleistocene glaciation in the Sierra Nevada and Basin ranges: Bulletin of
504 the Geological Society of America, v. 42, no. 4, p. 865-922.

Blaauw, M., Christen, J., 2011, Flexible paleoclimate age-depth models using an autoregressive gamma process: Bayesian Analysis, v. 6, no. 3, p. 457-474. doi:10.1214/11-BA618.

Blunt, A. B., and Negrini, R. M., 2015, Lake levels for the past 19,000 years from the TL05-4 cores, Tulare Lake, California, USA: Geophysical and geochemical proxies: Quaternary International, v. 387, p. 122-130

Benson, L., Kashgarian, M., Rye, R., Lund, S., Paillet, F., Smoot, J., Kester, C., Mensing, S., Meko, D., Lindstrom S., 2002, Holocene multidecadal and mullticentennial droughts affecting Northern California and Nevada: Quaternary Science Reviews, 21, 659-682.

Bowerman, N.D. and Clark, D.H., 2011, Holocene glaciation of the central Sierra Nevada,
508 California. Quaternary Science Reviews, vol. 30, no. 9-10, p. 1067-1085.

Bohacs, K.M., Carroll, A.R., Neal, J.E., and Mankiewicz, P.J., 2000, Lake-basin type, source potential, and hydrocarbon character: an integrated sequence-stratigraphic-geochemical framework, in: Lake basins through space and time: E.H. Gierlowski-Kordesch and K.R. Kelts, eds., AAPG studies in Geology v. 46, p. 3-34.

Brenner, M., Whitmore, T.J., Curtis, J.H., Hodell, D.A., Schelske, C.L. 1999. Stable isotope (δ13C and δ15N) signatures of sedimented organic matter as indicators of historic lake trophic state: Journal of Paleolimnology, v. 22, p. 205–221.

Brodie, C.R., Casford J.S,L., Lloyd J.M., Leng M.J., Heaton T.H.E., Kendrick C.P., 2012, Evidence for bias in C/N, δ13C and δ15N values of bulk organic matter, and on environmental interpretation, from a lake sedimentary sequence by pre-analysis acid treatment methods: Quaternary Science Reviews, v. 30 p. 3076–3087. doi: 10.1016/j.quascirev.2011.07.003

ter Braak, C.J., 1985, Correspondence analysis of incidence and abundance data: Properties in terms of unimodal response model: Biometrics, v. 41, p. 859-873.

Cayan, D., Tyree, M., Dettinger, M., Hidalgo, H., Tapash, D., Maurer, E., Bromirski, P., Graham, N., Reinhard, F. 2009. Climate Change Scenarios and Sea Level Rise Estimates

for California 2009 Climate Change Scenarios Assessment – Final Report: California Energy Commision, California Climate Change Center, p. 1-64.

Chiang, J.C.H., and Bitz, C.M., 2005, Influence of high latitude ice cover on the marine Intertropical Convergence Zone: Climate Dynamics, v. 25 n. 5, p. 477– 496. doi:10.1007/s00382-005-0040-5

Chiang, J.C.H., Lee, S., Putnam, A.E., Wang, X., 2014, South Pacific Split Jet, ITCZ shifts, and atmospheric North-South linkages during abrupt climate changes of the last glacial period: Earth and Planetary Science Letters, v. 406, p. 233-246.

Clark, D.H., 1997, A new alpine lacustrine sedimentary record from the Sierra Nevada: implications for Late-Pleistocene paleoclimate reconstructions and cosmogenic isotope production rates. EoS, Transactions, American Geophysical Union v. 78, 249.

Climate Resilience Toolkit: U.S. Federal Government, 2014: U.S. Climate Resilience Toolkit.

Cohen, A.S., 2003, Paleolimnology: New York, Oxford University Press Inc., p. 500.

Crowley, T.J., 2000, Causes of climate change over the past 1000 years: Science, v. 289, n. 5477, p. 270-277.

Davis, O. K., 1999, Pollen Analysis of a Late-Glacial and Holocene Sediment Core from Mono Lake, Mono County, California: Quaternary Research, v. 52, no. 2, p. 243-249.

Davis, O.K., Anderson, R.S., Fall, P., O'Rourke, M.K., Thompson, R.S., 1985, Palynological Evidence for early Holocene aridity in the Southern Sierra Nevada, California: Quaternary Research, v. 24, p. 322-332.

Erman, D.C., Andrews, E.D. and Yoder-Williams, M., 1988, Effects of winter floods on fishes in the Sierra Nevada. Canadian Journal of Fisheries and Aquatic Sciences, v. 45, no. 12, pp. 2195-2200.

Fites-Kaufman, J.A., Rundel, P., Stephenson, N., Weixelman, D., 2007, Montane and subalpine vegetation of the Sierra Nevada and Cascade Ranges, in: Terrestrial Vegetation of California, 3rd edition, eds. Barbour, M.G., Keeler-Wolf, T., Schroenherr, A.A, University of California Press, p. 456-493.

Gasiorowski, M., Sienkiewicz, E., 2013, The sources of carbon and nitrogen in mountain lakes and the role of human activity in their modification determined by tracking stable isotope composition: Water, Air, and Soil Pollution, v. 224, n. 4, doi: 10.1007/s11270-013-1498-0.

Gillespie, A.R., and Clark, D.H., 2011, Glaciations of the Sierra Nevada, California, USA: Developments in Quaternary Sciences, v. 15, p. 447-462.

Gillespie, I.G., and Loik, M.E., 2004, Pulse events in Great Basin Desert shrublands: physiological response of Artemisia tridentata and Purshia tridentata seedlings to increased summer precipitation: Journal of Arid Environments, V. 59, no. 1, p. 41-57.

Greene, D.C., and Stevens, C.H., 2002, Geologic Map of Paleozoic Rocks in the Mount Morrison Pendant, Eastern Sierra Nevada, California: California Department of Conservation,
Division of Mines and Geology. Mount Morrison Pendant, Sierra Nevada, California, MAP SHEET 53.

Grim, E., www.tiliait.com

Grimm, E., 1987, CONISS: a FORTRAN 77 program for stratigraphically constrained cluster analysis by the method of incremental sum of squares. Computers and Geosciences, v. 13, pp. 13-35.

Grimm, E., Maher J., Nelson, D., 2009, The magnitude of error in bulk-sediment radiocarbon dates from central North America. Quaternary Research. v 72, pp. 301-308. 10.1016/j.yqres.2009.05.006.

Haug, G. H., Hughen, K. A., Sigman, D. M., Peterson, L. C., Rohl, U., 2001, Southward migration of the Intertropical Convergence Zone through the Holocene: Science, v. 293, p. 1304-1308.

Herbst, D.B. and Cooper, S.D., 2010. Before and after the deluge: rain-on-snow flooding effects on aquatic invertebrate communities of small streams in the Sierra Nevada, California. Journal of the North American Benthological Society, v. 29, no. 4, pp.1354-1366.

Hodelka, B., McGlue, M., Zimmerman, S., Ali, G., Tunno, I., in review, Paleoproduction and environmental changes at Mono Lake (eastern Sierra Nevada) during the Pleistocene – Holocene transition: PALAEO, 2019.

IPCC, 2014, Climate Change 2014, Synthesis Report. Contribution of working groups I,II,III to the fifth assessment report of the Intergovernmental Panel of Climate Change. Core writing team Pachauri, R.K. and Meyer, L.A., IPCC, Geneva, Switzerland, p. 1-151.

Ivory, S.J., Lezine, A., Vincens, A., Cohen, A.S., 2018. Waxing and waning of forests: Late Quaternary biogeography of Southeast Africa: Global Change Biology, v. 24, p. 2939-2951.

Kirby, M. E., Knell, E. J., Anderson, W. T., Lachniet, M. S., Palermo, J., Eeg, H., Lucero, R., Murrieta, R., Arevalo, A., Silveira, E., and Hiner, C. A., 2015, Evidence for

insolation and Pacific forcing of late glacial through Holocene climate in the Central Mojave Desert (Silver Lake, CA): Quaternary Research, v. 84, no. 2, p. 174-186.

Kirby, M. E., Zimmerman, S. R. H., Patterson, W. P., and Rivera, J. J., 2012, A 9170-year record of decadal-to-multi-centennial scale pluvial episodes from the coastal Southwest United States: a role for atmospheric rivers?: Quaternary Science Reviews, v. 46, p. 57-65.

Lajoie, K., 1968, Late Quaternary Stratigraphy and Geologic History of Mono Basin, Eastern California. Dissertation, A.B., University of California.

Janbu, D., Aina & Paasche, Ø., Talbot, M.R., 2011, Paleoclimate changes inferred from stable isotopes and magnetic properties of organic-rich lake sediments in Arctic Norway: Journal of Paleolimnology, v. 46, pp. 29-44. 10.1007/s10933-011-9512-2.

Junak, S., Knapp, D.S., Haller, J.R., Philbrick, R., Schoener, A., Keeler-Wolf T., 2007 The California channel islands, in: Terrestrial Vegetation of California, 3rd edition, eds. Barbour, M.G., Keeler-Wolf, T., Schroenherr, A.A, University of California Press, p. 456-493.

Lyon, E., McGlue, M.M., Kim, S., Stone, J., Woolery, E., and Zimmerman, S., 2019, accepted.
Sublacustrine geomorphology and modern sedimentation in a glacial scour basin, June Lake, eastern Sierra Nevada USA: Journal of Sedimentary Research.

Loera, I., Sosa, V., Ickert-Bond, S.M., 2012, Diversification in North American arid lands: Niche conservatism, divergence and expansion of habitat explain speciation in the genus Ephedra: Molecular Phylogenetics and Evolution, v. 65, n. 2, 437-450.

Maciolek, J.A. and Needham, P.R., 1952. Ecological effects of winter conditions on trout and trout foods in Convict Creek, California, 1951. Transactions of the American Fisheries Society, v. 81 no. 1, p. 202-217.

Mackie E.V., Leng M.J., Lloyd J.M., Arrowsmith C., 2005, Bulk organic $\delta^{13}C$ and C/N ratios as palaeosalinity indicators within a Scottish isolation basin. Journal of Quaternary Science. v. pp. 303–312. doi: 10.1002/jqs.919.

Mann, M.E., Bradley, R.S., Hughes, M.K., 1999, Northern hemisphere temperatures during the past Millennium: Inferences, uncertainties, and limitations: Geophysical Research Letters, v. 26, n. 6, p. 759-762.

McFadden, M.A., Mullins, H.T., Patterson, W.P. and Anderson, W.T., 2004, Paleoproductivity of eastern Lake Ontario over the past 10,000 years: Limnology and Oceanography, *49*(5), p. 1570-1581.

McGlue, M.M., Ellis, G.S. and Cohen, A.S., 2015, Modern muds of Laguna Mar Chiquita (Argentina): Particle size and organic matter geochemical trends from a large saline lake in the thick-skinned Andean foreland. Geological Society of America Special Papers, v. 515, p. 1-18.

McGlue and Woolery, in review, High resolution CHIRP seismic profiling reveals basin floor morphology and shallow stratigraphy and Convict Lake. Quaternary International, 2019.

McGlue, M.M., Woolery, E.W., Black, M., Ivory, S.J., Alimayahi, A., Zimmerman, S., Deglacial sedimentary history of Convict Creek valley, eastern Sierra Nevada (California, USA)

Melack, J.M., Stoddard, J.L. and Ochs, C.A., 1985, Major ion chemistry and sensitivity to acid
precipitation of Sierra Nevada lakes. Water Resources Research, v. 21, no. 1, p. 27-32.

Mensing, S.A., Benson, L., Kashgarian, M., Lund, S., 2004, A Holocene pollen record of persistent drought from Pyramid Lake, Nevada, USA: Quaternary Research, v. 62, p. 29-38.

Mensing, S. A., Sharpe, S. E., Tunno, I., Sada, D. W., Thomas, J. M., Starratt, S., Smith, J., 2013, The Late Holocene Dry Period: multiproxy evidence for an extended drought between 2800 and 1850 cal yr BP across the central Great Basin, USA: Quaternary Science Reviews, v. 78, p. 266-282

Meyers, P.A., and Teranes, J.L., 2001, Sediment organic matter, in Last, W.M., and Smol, J.P., ed., Tracking environmental change using lake sediments: Dordrecht, Netherlands, Kluwer Academic Publishers, v. 2, p. 239- 269.

Meyers, P.A., and Ishiwatari, R., 1993, Lacustrine organic geochemistry – an overview of indicators of organic matter sources and diagenesis in lake sediments: Organic Geochemistry, v. 20, no. 7, p. 867-900.

Mono County Community Development Department (MCCDD), 2007, Upper Owens River Water Shed Assessment, p. 1-155.

Moss, B., 1973, The influence of environmental factors on the distribution of freshwater algae – an experimental study – the role of pH and the carbon dioxide – bicarbonate system: Journal of Ecology, v. 61, p. 157-177/

National Oceanic and Atmospheric Administration (NOAA), Global Climate Perspectives System, Monthly Station - Mammoth Lakes Ranger Station, 2018.

Noble, P.J., Ball, G.I., Zimmerman, S.H., Maloney, J., Smith, S.B., Kent, G., Adams, K.D., Karlin, R.E., and Driscoll, N., 2016, Holocene paleoclimate history of Fallen Leaf

Lake, CA., from geochemistry and sedimentology of well-dated sediment cores: Quaternary Science Reviews, v. 131, p. 193-210.

Negrini, R. M., Wigand, P. E., Draucker, S., Gobalet, K. W., Gardner, J. K., Sutton, M. Q., Yohe, R. M., II, 2006, The Rambla highstand shoreline and the Holocene lake-level history of Tulare Lake, California, USA: Quaternary Science Reviews, v. 25, p. 1599-1618.

Newton, M.S., 1994, Holocene fluctuations of Mono Lake, California: The sedimentary record: Society for Sedimentary Geology Special Publication, v. 50, p. 143-157.

North, M., Collins, B., Safford, H., Stephenson, N., 2016, Montane Forests, in Ecosystems of California, eds. Mooney, H., and Zavaleta, E., University of California Press, p. 553-573.

O'Kapp, R., 2000, Pollen and Spores: American Association of Stratigraphic Palynologists Foundation, 2nd edition, p. 1-279.

O'Keefe, J. M. K., and Wymer, C. L., 2017, An Alternative to Acetolysis: Application of an Enzyme-Based Method for the Palynological Preparation of Fresh Pollen, Honey Samples and Bee Capsules: American Association of Stratigraphic Palynologists. Palynology, v. 41, no. 1, p. 117-120.

O'Neil, J.M., Davis, T.W., Burford, M.A., Gobler, C.J., 2012, The rise of harmful cyanobacteria blooms: the potential roles of eutrophication and climate change: Harmful Algae, v. 14, p. 313–334.

Phillips, F.M., Zreda, M., Plummer, M.A., Elmore, D., Clark, D.H., 2009, Glacial geology and chronology of Bishop Creek and vicinity, eastern Sierra Nevada, California Geological Society of America Bulletin, v. 121, p. 1013–1033.

Pöschke, F., Lewandowski, J., Engelhardt, C., Preuß, K., Martin Oczipka, M., Ruhtz, T., Kirillin, G., 2015, Upwelling of deep water during thermal stratification onset – a major mechanism of vertical transport in small temperate lakes in spring: Water Resources Research, v. 51, n. 12, pp. 9612-9627.

Piovono, Ed., and Ariztegui, D., 2004, Stable isotopic record of hydrological changes in subtropical Laguna Mar Chiquita (Argentina) over the last 230 years: The Holocene, v. 14 n. 4, p. 525-535.

Reimers, N., Maciolek, J.A., Pister, E.P., 1955, Limnological Study of the Lakes in Convict Creek Basin, Mono County, California: United States Department of the Interior, Fish and Wildlife Service. Fishery Bulletin 153, p. 1-72.

Richardson, R., 2002, Economic Benefits of Wildlands in the Eastern Sierra Nevada Region of California: The Wilderness Society.

Smol, J.P., Wolfe, A.P., Birks, J.B., Douglas, M.S.V., Jones, V.J., Korhola, A., Pientiz, R., Ruhland, K., Srovari, S., Antoniades, D., Brooks, S.J., Fallu, M.A., Hughes, M., Keatley, B.E., Laing, T.E., Michelutti, N., Nasarova, L., Nyman, Marjut, Paterson, A.M., Perren, B., Quinlan, R., Rautio, M., Saulnier-Talbot, E., Siitonen, S., Solovieva, N., Weckstrom, J., 2005, Climate-driven regime shifts in the biological communities of arctic lakes: Proceedings of the national academy of Sciences of the United States of America, v. 102, n. 12, p. 4397-4402.

Stevens, P.F., Luteyn, J., Oliver, E.G.H., Bell, T.L., Brown, E.A., Crowden, R.K., George, A.S., Jordan, G.J., Ladd, P., Lemson, K., McLean, C.B., Menadue, Y., Pate, J.S., Stace, H.M., Weiller, C.M., 2004, Ericaceae: In. Flowering Plants. Dicotyledons: Celastrales, Oxalidales, Rosales, Cornales, Ericales. The families and genera of vascular plants, ed. Kubitzki, K., Springer, v. 6, p. 145–194. ISBN 9783540065128

Stine, S., 1990. Late Holocene Fluctuations of Mono Lake, eastern California: Paleogeography, Paleoclimatology, Palaeoecology. v. 78, P. 333-381.

Talbot, M.R., and Johannessen, T., 1992, A high resolution palaeoclimatic record for the last 27,500 years in tropical West Africa from the carbon and nitrogen isotopic composition of lacustrine organic matter. Earth and Planetary Science Letters, v. 110, p. 23-37.

Taranu, Z.E., Zurawell, R.W., Pick, F., Gregory-Eaves, I, 2012: Predicting cyanobacterial dynamics in the face of global change: the importance of scale and environmental context. Global Change Biology v. 18, p. 3477–3490.

Taranu. Z.E., Gregory-Eaves, I., Leavitt, P.R., Bunting, L., Buchaca, T., Catalan J., Domaizon, I., Guilizzoni, P., Lami, A., McGowan, S., Moorhouse, H., Morabito, G., Pick, F.R., Stevenson, M.A., Thompson. P.L., Vinebrooke, R.D., 2015, Acceleration of cyanobacterial dominance in north temperate-subarctic lakes during the Anthropocene: Ecology Letters, v. 18, n. 4. doi: https://doi.org/10.1111/ele.12420

Vreča, P. and Muri, G., 2010, Sediment organic matter in mountain lakes of north-western Solvenia and its stable isotopic signatures: records of natural and anthropogenic impacts. Hydrobiologia, v. 648, p. 35-49.

Wetzel, R.G., 2001, Limnology (3rd ed): San Diego, Academic Press, p. 1006

Zimmerman, S. R., S. R. Hemming, S. Starratt, Holocene sedimentary architecture and paleoclimate variability at Mono Lake, CA. In revision, Feb. 2018 for GSA Special Paper 536, From Saline to Freshwater: The Diversity of Western Lakes in Space and Time; Starratt, S.W. and Rosen, M. R., eds.

Zong, Y., Lloyd J.M., Leng M.J., Yim W.W.S., Huang, G., 2006, Reconstruction of Holocene monsoon history from Pearl River Estuary, southern China, using diatoms and carbon isotope ratios: The Holocene, v. 16, pp. 251–263. doi: 10.1191/0959683606hl911rp.

VITA

EDUCATION

Master of Science, University of Kentucky, expected 2019

Bachelor of Science, Morehead State University, awarded 2017

PROFESSIONAL HISTORY

Project Manager, Ledcor

Project Coordinator, Ledcor

Teaching Assistant, University of Kentucky

Geoscientist, National Park Service, John Fossil Beds National Monument

Invertebrate Paleontology Intern, American Museum of Natural History

Undergraduate Research Fellow, Morehead State University

AWARDS

Outstanding Senior in Geology, 2017

AASP, American Association of Stratigraphic Palynologists – Best Student Paper, 2015